THE UNIVERSITY OF MANITOBA

MEASUREMENT OF WALL SHEAR STRESS WITH HOT WIRE ANEMOMETER

by

Sheikh Burhanuddin

A THESIS

SUBMITTED TO THE FACULTY OF GRADUATE STUDIES

IN PARTIAL FULFILLMENT OF THE REQUIREMENTS FOR THE DEGREE

OF MASTER OF SCIENCE IN ENGINEERING

DEPARTMENT OF MECHANICAL ENGINEERING

WINNIPEG, MANITOBA

August, 1980

MEASUREMENT OF WALL SHEAR STRESS WITH HOT WIRE ANEMOMETER

BY

SHEIKH BURHANUDDIN

A thesis submitted to the Faculty of Graduate Studies of the University of Manitoba in partial fulfillment of the requirements of the degree of

MASTER OF SCIENCE

ABSTRACT

Shear stress measurement at the wall in a boundary layer and in a diffuser flow with a hot wire anemometer is described. The effect of the proximity of the wall on hot wire measurements is discussed and a simple and quite satisfactory method of correction of wall proximity effect is suggested. The correction was originally developed in boundary layer flow (developed on the walls of a pipe) and compared with published data from similar flows. It was found satisfactory and in turn was extended to diffuser flow.

The Preston tube was used to measure shear stress at the wall in a diffuser flow using Patel's calibration. Furthermore, these measurements were corrected by using Frei & Thomann's correction which was developed by using a sealed floating element technique in an adverse pressure gradient. These results agree very well with the measurements made with a hot wire anemometer.

Some quantities, like boundary layer parameters, turbulence intensity, and skewness and flatness of u and $\partial u/\partial t$, were measured to specify the flow in which the effect of the wall proximity on hot wire readings was studied and corrected. The relationship between skewness and flatness of $\partial u/\partial t$ established by Van Atta & Antonia is also valid

in the flows investigated here.

The sub-layer next to the wall exists in all flows (i.e., with different types of pressure gradients) and the velocity in this region is linear. This layer extends to a value of Y^+ approximately equal to 5. Even in turbulent flow, $\tau_w = \mu \left| \partial \bar{U} / \partial Y \right|_w$ is valid. Now the characteristics of the sub-layer are,

(a) Intensity of turbulence is maximum at the edge of the sub-layer (i.e., at $Y^+ = 5$).

(b) The skewness of $\partial u / \partial t$ decreases in the sub-layer towards the wall.

(c) The flatness of $\partial u / \partial t$ goes very high towards the wall.

ACKNOWLEDGEMENTS

The author wishes to thank Professor R.S. Azad (Thesis Advisor) for his guidance, helpful discussions and appreciation during this work. Thanks are also due to Professor J. Tinkler for reviewing this thesis.

The assistance provided by Mr. Ken Tarte in experimental setup and Mrs. P. Giardino in typing the thesis is appreciated.

Special thanks are due to my mother for her patience and encouragement.

TABLE OF CONTENTS

LIST OF FIGURES

LIST OF TABLES

NOMENCLATURE

$B(u)$	Probability density of u
C_f	Coefficient of friction, $2\left[\frac{U^*}{U_\infty}\right]^2$
d	Outer diameter of Preston Tube
D	Diameter of pipe
E	Voltage
$E(R, 0, \infty)$	The voltage with resistance R, velocity zero away from the wall
$E(R', 0, Y)$	The voltage with resistance R', velocity zero at distance Y
E_p	Energy peak
F	Flatness factor
H	Shape factor, δ_1/δ_2
L	Turbulent eddy length scale
m	Slope of a straight line
P_{st}	Static pressure measured with respect to atmosphere
R	Radius of pipe
r	Variable radius
Re	Reynolds Number, $Re_{av.} = \frac{U_{av}D}{\nu}$
	$Re_\infty = \frac{U_\infty D}{\nu}$, $Re_\delta = \frac{U_\infty \delta}{\nu}$
	$Re_{\delta_1} = \frac{U_\infty \delta_1}{\nu}$, $Re_{\delta_2} = \frac{U_\infty \delta_2}{\nu}$
S	Skewness factor
T	Time scale, $T = \int_0^T d(t)$
t	Time

U_{av}	Average velocity
U_{cl}	Centre line velocity
U_{∞}	Free stream velocity
$\bar{U}$	Time averaged local mean velocity
U^+	Non-dimensional velocity, $\frac{\bar{U}}{U^*}$
U^*	Friction velocity, $\left\|\frac{\tau_w}{\rho}\right\|^{\frac{1}{2}}$
U^+_{unc}	Non-dimensional uncorrected velocity, $\frac{\bar{U}_{unc}}{U^*}$
ΔU^+_{unc}	Deviation of U^+_{unc} from $U^+ = Y^+$ curve
$\tilde{u}(t)$	Instantaneous velocity
u	Longitudinal or tangential component of turbulent velocity
u'	Root mean square of u, $[\bar{u}^2]^{\frac{1}{2}}$
v	Normal component of turbulent velocity
Y	Distance from the wall
Y_{unc}	Uncorrected distance measured from the wall
Y^+	Non-dimensional distance, $\frac{YU^*}{\nu}$
Y^+_{unc}	Non-dimensional uncorrected distance, $\frac{Y_{unc}U^*}{\nu}$
ρ	Density of air
τ_w	Shear stress at the wall
ν	Kinematic viscosity, μ/ρ
μ	Dynamic visocisty
δ	Boundary layer thickness at 99% of U_{∞}
δ_o	Sub-layer thickness

δ_1	Displacement thickness
δ_2	Momentum thickness
Δ	Difference
ϵ	Energy loss occurring in the flow
$\partial/\partial t$	Derivative with respect to time

Subscripts

av	Average
cc	Contraction cone
∞	Away from the wall, free stream
cr	Critical
tur	Turbulent or eddy
w	Wall

Superscript

-	Time averaged

1.0 INTRODUCTION

In an adverse pressure gradient, no conclusive method has yet been outlined to measure the shear stress at the wall. One example of an adverse pressure gradient is diffuser flow. For presenting results of turbulent flow close to the wall in a diffuser, the wall velocity scale (i.e., friction velocity), is required. The friction velocity, U^*, can be obtained from the shear stress at the wall. By definition,

$$\tau_w = \mu \left| \partial \bar{U} / \partial Y \right|_w$$

since $\mu = \rho\nu$

$$\tau_w/\rho = \nu \left| \partial \bar{U} / \partial Y \right|_w$$

now $\tau_w/\rho = (U^*)^2$,

therefore

$$(U^*)^2 = \nu \left| \partial \bar{U} / \partial Y \right|_w \quad .$$

The shear stress at the wall is proportional to the velocity gradient at the wall. The velocity gradient at the wall is obtained by measuring the mean velocity at several positions close to the wall. The mean velocity can, of course, be measured with a Pitot tube but the sub-layer adjacent to the wall is so thin as compared to the dimensions of the Pitot tube that it is impossible to measure mean velocity with a Pitot tube at several positions within the sub-layer. Another difficulty in measuring mean velocity with a Pitot tube is the

very small magnitude of dynamic pressure in the sub-layer which is hard to measure even with a precise micro-manometer. The aerodynamic effect is also a drawback. Therefore a hot wire anemometer was to be used to measure mean velocity close to the wall in the diffuser flow. The boundary layer type of hot wire probe can get very close to the wall. When the tips of the prongs of this probe are just at the wall (but not touching it), the distance of the hot wire from the wall is 0.06 mm (approximately). Therefore the mean velocity can be measured with the hot wire anemometer at several positions in the sub-layer.

Hot wire readings obtained very close to the wall must be corrected because the proximity of a solid boundary, having much higher thermal conductivity than the fluid, affects the heat loss from the hot wire. The boundary is effectively at ambient air temperature so additional heat is extracted from the fluid that is heated by the wire. Therefore, a higher than actual velocity is indicated by the anemometer. The effect increases rapidly as the wire approaches the wall. This effect is typically limited to within 0.5 mm from the wall. The wall conduction effect has been observed by many workers and some have attempted to correct hot wire readings in the proximity of the wall.

In 1924, Van Der Hegge Zijnen obtained a correction by measuring the total heat loss from the wire at a large

distance from the wall, and at various closer distances from the wall, all the measurements being taken in still air. The extra heat loss so obtained was then used to correct experimental velocity measurements. The same method was used by Dryden (1936) and Weissberg (1956). Reighardt (1940) calibrated hot wires close to the wall in a laminar flow channel and used this calibration in a channel with a turbulent flow having the same value of wall shear stress. Wills (1962) and Ueda & Hinze (1975) used the same method. This method is limited to the measurement of turbulent flows whose friction velocities are within the range of the laminar flow friction velocities used for calibration.

Oka and Kostic (1972) and Zemkaya et al. (1979) formulated a method to find the friction velocity at the wall. This method assumes the existence of the linear law of velocity, i.e., $U^+ = Y^+$. According to this method, an uncorrected U^+ vs. Y^+ graph is plotted using U^* from some other approximate method and the Y^+_{unc} value corresponding to the minimum position in this graph is noted. Then the uncorrected $\bar{U}$ vs. Y graph is drawn and the Y_{unc} value corresponding to the minimum position in this graph is noted. Then U^* is calculated as follows:

$$Y^+_{unc} = \frac{Y_{unc} U^*}{\nu} \quad ,$$

or

$$U^* = \frac{Y^+_{unc} \nu}{Y_{unc}} \quad .$$

This method requires a friction velocity from some other method such as the Log Law. But once the shear stress is known and, since the velocity profile is linear and passes through the origin ($\bar{U} = 0$, $Y = 0$), it does not require any other method to obtain the true mean velocity near the wall.

Chauve (1977) used two methods of correction of hot wire measurements very close to the wall. The first method was similar to that used by Van Der Hegge Zijnen (1924) described earlier. According to the second method, in the absence of the flow, the resistance of the anemometer is adjusted for each distance Y from the wall such that the voltage remains equal to that far away from the wall. If $E(R, \bar{U}, Y)$ is the voltage E at resistance R, velocity $\bar{U}$ at distance Y then,

$$E(R, 0, \infty) = E(R', 0, Y)$$

In the presence of flow, the voltage measured corresponding to the adjusted resistance R' at a distance Y from the wall is equal to the voltage measured corresponding to resistance R for the same velocity at an infinite distance from the wall. This voltage is converted into velocity using the calibration curve. This method can introduce considerable errors in measurements because a probe calibration at all resistance settings is required.

The present method of correction is similar to that used by Van Der Hegge Zijnen (1924) except that the hot wire

output is linearized. It consists of traversing a boundary layer type of probe through the region of wall proximity effect (about 1 mm thick) with and without flow. The voltage at each location from the wall for each condition is noted. The true velocity is obtained by subtracting no flow voltage from the flow voltage.

The correction should be developed in a flow in which the friction velocity is already known so that the corrected friction velocity could be compared with it before applying the correction to the diffuser flow. A boundary layer flow or a developing flow in a pipe (in which the wall region has the characteristics of a boundary layer) can be used for this purpose because the Log. Law is applicable in this flow, and the cross-plot method can be applied to the Log. Law for getting the friction velocity. The corrected friction velocity measurements obtained by Ueda and Hinze (1975) in a boundary layer flow can also be used for comparison in the same velocity (free stream) range.

Considering the available facilities, the correction would be developed in a developing pipe flow and after comparing the results with the available data, it would be applied to the diffuser flow.

In a diffuser flow the shear stress at the wall can also be measured with a Preston tube using Patel's calibration (1965). Recently Frei and Thomann developed a method for

correcting Patel's calibration in an adverse pressure gradient. They used a sealed floating element technique for this purpose. The friction velocity obtained from corrected Preston tube measurements in a diffuser flow were to be used for comparing the corrected hot wire measurements in the same flow.

2.0 THEORETICAL CONSIDERATIONS

The central idea of the following discussion of boundary layer structure has been taken from Levich (1962).

The steady advance of a fluid in spearate layers is known as laminar flow. The unsteady chaotic motion in which the flow velocity fluctuates about some average value is known as turbulent flow. At a certain value of the Reynolds number (Re_{cr}), steady laminar flow gives way to distinctly unsteady, chaotic motion in which only on a time average is there net flow in a particular direction. The gross over all motion of a fluid is subject to infinitesimal disturbances. At $R_e < Re_{cr}$, disturbances that occur in the fluid are rapidly damped. At $Re > Re_{cr}$, disturbances are not damped, but rather reinforce each other and result in a chaotic regime having random eddies superposed on the basic motion. At $Re >> Re_{cr}$ eddy velocities of extremely varied magnitude are superposed upon the motion of a fluid having a local mean velocity, say, $\bar{U}$. Turbulence eddies may be characterized by their velocities and by the distances over which these velocities change significantly. These distances are known as the scale of motion. Let $\Delta\bar{U}$ be the change in the average velocity over a distance equal to the scale of an eddy L. Thus for the example of turbulent motion in a tube, the largest scale L of turbulence eddies is equal to the diameter of the tube and the eddy velocities vary within the range of average

velocity over that distance; i.e., they are of the order of the maximum value of the velocity at the centre of tube.

Such large scale eddies contain the main part of the kinetic energy of turbulent motion. Together with these large scale eddies, turbulent flow also includes eddies of smaller scales and lesser velocities. With a large quantity of small scale motion, there is a considerable dissipation of energy, which is transformed to heat. Small scale motions serve as a bridge by means of which the kinetic energy of large motions may be converted into thermal energy. Although turbulent motion occurs only at relatively high Reynolds numbers, it is accompanied by considerable dissipation of energy. From this standpoint it is possible to define a certain effective eddy viscosity, μ_{tur}, appropriate to turbulent flow. This eddy viscosity expresses energy losses occurring in the flow per unit time per unit volume by the equation

$$\varepsilon = \mu_{tur} (\Delta\bar{U}/L)^2 \quad . \qquad (1)$$

ε is not a function of the scale of the motion but is a characteristic constant for a given flow. In particular, for the largest scale motions, it equals the energy dissipated in the process of creating smaller scale motions. This process occurs at high Reynolds numbers and cannot be a function of the molecular viscosity μ of the fluid.

Therefore ε must be determined from the quantities characteristic of large scale turbulent motion. These include the velocity $\Delta\bar{U}$, the scale of motion L and density of the fluid ρ. These quantities can be combined into a single quantity with the same dimensions as ε.

$$\varepsilon \approx \rho \frac{(\Delta\bar{U})^3}{L} \quad . \tag{2}$$

There from (1) and (2)

$$\mu_{tur} \approx \rho \, \Delta\bar{U} L \quad . \tag{3}$$

Following the analogy between turbulent motion and random motion of gas molecules, the scale of motion L may be considered as the analog of the length of the mean free path, and the eddy velocity as the analog of the average velocity of the gas molecules. Therefore the approximation for the eddy viscosity can be written as $\Delta\bar{U} \approx L(\partial\bar{U}/\partial L)$. With the aid of μ_{tur}, the shear stress can be defined,

$$\tau \approx \mu_{tur} (\partial\bar{U}/\partial L) \approx \rho L^2 (\partial\bar{U}/\partial L)^2 = \alpha\rho L^2 (\partial\bar{U}/\partial L)^2 \tag{4}$$

where α is a constant.

Now consider turbulent flow past a flat plate of infinite extent downstream in the plane Y = 0. Let the mean flow be

in the x-direction and the time average velocity be $\bar{U}$. The average velocity is, in general, a function of the distance of the fluid layer from the surface of the solid body, and thus $\bar{U} = \bar{U}(Y)$. The function $\bar{U}(Y)$ can be obtained by re-writing equation (4) in the form

$$\partial\bar{U}/\partial L = (\tau/\rho\alpha)^{\frac{1}{2}} (1/L) \quad . \tag{5}$$

In order to integrate the above equation it is necessary to determine the scale of the motion as a function of the distance Y separating the fluid layer from the solid surface. The conditions determining the flow field over a flat plate of infinite extent do not include the dimensions of the body which could be used to describe a characteristic scale of large turbulence eddies L. It is logical, therefore, to assume that

$$L \approx Y \quad . \tag{6}$$

Now equation (5) can be written as

$$\partial\bar{U}/\partial Y = 1/(\alpha)^{\frac{1}{2}} (\tau/\rho)^{\frac{1}{2}} (1/Y) \ .$$

Let $(\tau/\rho)^{\frac{1}{2}} = U^*$, the friction velocity, and introduce the dimensionless velocity $U^+ = \bar{U}/U^*$ and dimensionless distance $Y^+ = (YU^*/\nu)$ so that

$$dU^+/dY^+ = 1/(\alpha^{\frac{1}{2}}Y^+) \quad .$$

Integrating the above equation gives

$$U^+ = \ell_n Y^+/\alpha^{\frac{1}{2}} + C \quad . \qquad (7)$$

The values of the constants α and C must be determined experimentally. Equation (7) is usually written as

$$U^+ = A\ \ell_n Y^+ + B \quad .$$

Various experimental measurements of velocity distribution show that the logarithmic relationship is valid only for $Y^+ \geq 30$. The upper limit of Y^+ depends on the Reynolds number.

The reduction in the scale of turbulence eddies as the wall is approached is matched by a corresponding reduction in the Reynolds number,

$$Re = (U^*L/\nu) \quad .$$

The friction velocity U^* is the velocity of turbulence eddies that are characteristic of the flow. At a certain $L = \delta_o$, Re is approximately equal to unity. In the region $Y < \delta_o$, known as the viscous sub-layer, the effects of viscosity are such as to give Newtonian flow. The thickness of the viscous sublayer is given by the condition

$(U^* \delta_o/\nu) \approx 1$. Two hypotheses regarding the velocity distribution in the viscous sub-layer have been suggested:

1) The Prandtl (1952) hypothesis, which has been accepted widely, states that in the region $Y < \delta_o$, the fluid motion is entirely laminar. Prandtl named this region the laminar sub-layer. The shear stress τ in the laminar sub-layer evidently may be expressed by the equation

$$\tau = \rho\nu(d\bar{U}/dY) \quad . \tag{8}$$

The velocity distribution can, therefore, be expressed by the linear equation

$$\bar{U} = (\tau/\rho\nu)Y + C \quad .$$

The integration constant must be equal to zero, since the velocity of the fluid at the solid surface is zero. Therefore, for $Y < \delta_o$,

$$\bar{U} = (\tau/\rho\nu)Y \quad .$$

$$\frac{\bar{U}}{(\tau/\rho)^{\frac{1}{2}}} = (\tau/\rho)^{\frac{1}{2}} (Y/\nu)$$

$$U^+ = Y^+ \quad . \tag{9}$$

Therefore, for the case of turbulent flow past a solid plane, the flow can be divided into three regions:

(a) a region of turbulent flow, (b) a buffer layer, and (c) a laminar sub-layer.

2) The other hypothesis presented by Landau and Levich (1959) states that the turbulent motion in the viscous sub-layer does not suddenly disappear but is gradually damped as it approaches the wall. The dependence of L on Y can no longer be applied on the basis of dimensional consideration, as is the case for the region of developed turbulence. All quantities in the viscous sub-layer may be functions of viscosity, and the distance from the wall is no longer the sole quantity with a linear dimension. The distribution of the average velocity in this layer has the same form as in laminar flow, i.e.,

$$U_x \sim Y$$

where U_x is the x-component of fluid velocity U. Although turbulence eddies do not originate in the viscous sub-layer, they enter it from the side $Y > \delta_o$. The eddy velocities have the same magnitude as the average velocities in the sub-layer. Therefore,

$$u \sim Y$$

In view of the continuity equation

$$\frac{\partial u}{\partial x} + \frac{\partial v}{\partial y} = 0$$

The normal component of eddy velocity is

$$v = - \int \frac{\partial u}{\partial x} \, dY \sim Y^2 \quad .$$

The proportionality coefficient in the expression for v can be evaluated using the condition that, at $Y \approx \delta_o$, the eddy velocity v at the boundary of the viscous sub-layer is of the same order of magnitude as the characteristic velocity of the turbulent flow U^*. Therefore,

$$v = (U^* \, Y^2/\delta_o^{\,2}) \quad .$$

Thus, in a viscous sub-layer the tangential and normal components of the average velocity and of the eddy velocities vary as a function of distance in the same way as the distribution of velocities in a laminar boundary layer. This, in essence, is the extent of the resemblance between a viscous sub-layer and a laminar boundary layer.

On the basis of the above discussion and experimental measurements, the turbulent boundary layer can be divided into three regions. In $Y^+ \leq 5$, region, the dimensionless velocity (U^+) is equal to the dimensionless distance (Y^+).

This region is called the viscous sub-layer. This layer is very thin and exists adjacent to the wall. In this region the shear stress contribution from turbulent friction may be neglected compared with molecular friction. The velocity gradient is steepest and constant in this layer. In the region $5 \leq Y^+ \leq 30$ the molecular and turbulent friction are of the same order of magnitude. This region is called the mixing or buffer layer. In the $Y^+ \geq 30$ region the molecular contribution is negligible compared with the turbulent friction. This region is called the turbulent core. A logarithmic curve [Equation (7)] fits the data well in this region. The complete universal profile is given by:

$Y^+ \leq 5$	$U^+ = Y^+$
$5 \leq Y^+ \leq 30$	Mixing
$Y^+ \geq 30$	$U^+ = A \ell_n Y^+ + B$.

There is a small amount of scatter in the values of the constants A and B in the Log. Law. Some experimentalists have suggested the following values of the constants A and B:

A	B	Investigator
2.44	4.9	Clauser (1956)
2.44	5.85	Townsend (1956)
2.5	5.1	Coles (1955)
2.7	4.5-6.0	Comte-Bellot (1965)

The suggestion of a possible slight dependence of A & B on Reynolds number has been made [Hinze (1962), Comte-Bellot (1965)] but it is not confirmed yet.

Cross-Plot Method:

This method can be used to calculate the friction velocity, U^*, from the Log. Law, and the measured velocity profile in the turbulent core region of the boundary layer.

According to this method, a value of Y^+ is assumed in the range where the Log. Law is applicable, say, $30 \leq Y^+ \leq 100$. By putting this value of Y^+ in the Log. Law we can calculate the corresponding value of U^+. Then the product of U^+ and Y^+ is calculated.

$$U^+Y^+ = \frac{\bar{U}}{U^*} \cdot \frac{YU^*}{\nu} = \frac{\bar{U}Y}{\nu} \quad .$$

So $\frac{\bar{U}Y}{\nu}$ = a numerical value. Now from the above equation $\bar{U}$ is plotted against Y on a linear graph. On the same graph the measured velocity profile is plotted and the value of $\bar{U}$ at the inter-section of the two curves is noted. This value of $\bar{U}$ is divided by the value of U^+ obtained in the first step. The resulting value is the friction velocity U^*. Several values of Y^+ in the applicable range of the Log. Law are selected and U^* is calculated in the manner describe above. These values should be very close if the velocity profile measurements are correct and Y^+ lies in the applicable range.

APPENDIX:

The boundary layer thickness, displacement thickness, momentum thickness, skewness factor and flatness factor have been defined in the appendix.

3.0 EXPERIMENTAL FACILITIES AND EQUIPMENT

The experimental facility and the equipment used in the research are described in this section.

3.1 BOUNDARY LAYER FACILITIES

The boundary layer developed on the wall of a pipe was studied in an open-return type low speed wind tunnel. This wind tunnel has been described by Trupp (1973). It is an excellent facility for studying boundary layer flow. A gunmetal pipe of very smooth inner surface and of 27.0 cm inner diameter and 2.65 meter length was attached to the circular contraction cone of area ratio 16:1. Tripping paper number 16 was pasted to the first 27 cm length of the pipe for thickening the boundary layer. This type of tripping was first studied by Klebanoff & Diehl (1952). The measuring station was selected at 2.22 meter from the tripping. It was well inside the pipe (15 cm from the exit) to be free from end effects. It was confirmed by observing no change in the free stream velocity 3 cm downstream from the measuring station.

The surface of the boundary layer fluctuates outward upto 1.2 times the boundary layer thickness, δ. The potential flow region was almost three times of 1.2 δ so there was no chance of any boundary layer interaction from the opposite sides. But no consideration was given to the

condition that δ should be small as compared to the pipe radius for a pipe boundary layer to be classed as a plane boundary layer. This tunnel can generate free stream velocities from 2 ms^{-1} to 13 ms^{-1} on the centreline at the measuring station. Required free stream velocities were obtained by adjusting the fan power and measuring the pressure drop across the contraction cone which was calibrated with a Pitot tube in terms of free stream velocity on the centreline at the measuring station. The pressure across the contraction cone was measured with a 0 - 0.5 inch water gauge inclined manometer (Airflow Developments).

The probe traversing mechanism for this tunnel consisted of a co-ordinate table, (Model FB102, M.S. Tool Supplies) having longitudinal feed of 37 cm and cross-feed of 15 cm, and a micro-stage which could slide on the co-ordinate table. A digit micrometer head (dual directional counter type, Mitutoyo Mfg.) having 0.01 mm graduation and 0 - 25 mm range was used to slide the micro-stage on the table along the horizontal diameter of the pipe. A vertical slide attached to the micro-stage was used to hold the tube for supporting the probe. Backlash in the micrometer was measured and care was taken to eliminate it from distance measurements. The co-ordinate table was kept in a horizontal position by using balancing weights and a spirit level.

3.2 DIFFUSER FACILITIES

The wind tunnel for studying the diffuser flow has been described by Azad & Hummel (1971) and Okwuobi & Azad (1973). A seventy-three diameters long steel pipe of inside diameter 10.16 cm was used to feed fully developed flow into the diffuser. The settling chamber, 92 cm in diameter and 3.66 m long was provided with two sets of fine mesh screens. The circular contraction cone with an area ratio of 89:1 was fabricated from plywood. The diffuser was machined from cast aluminum (see Figure 1 for geometry). Static pressure holes of 0.6 mm diameter and spaced 90° apart were drilled at intervals of 6 cm along the wall of the diffuser. The reference station for the tunnel calibration was selected at 77 cm upstream from the exit of the diffuser (5 cm inside the pipe) and at a quarter radius from the wall of the pipe because the mean bulk velocity is obtained at this position in fully developed pipe flow. The pressure across the contraction cone was measured with a 0 - 8.0 inch, 0.827 specific gravity fluid Inclined Manometer (Trimount Instruments).

The traversing mechanism for this wind tunnel consisted of a co-ordinate table (same as described earlier) attached to a circular milling table (for angle setting) and a micro-stage which could slide on the co-ordinate table. The digit micrometer, vertical slide and balance weights were the same as described earlier for the boundary layer tunnel. The

circular milling table enabled the probe to be moved at any angle to the wall or axis of the diffuser.

3.3 INSTRUMENTATION

Electronic and mechanical instruments were used for this research.

The mean static pressure along the diffuser wall was measured with a static pressure tube of 1.2 mm outer diameter (United Sensor, U.S.A., USC-E-120-04) and found to be the same as measured with wall static pressure taps. Velocity measurements for the hot wire probe calibration were obtained with a static pressure tube (as described above) and a Pitot tube of 1.2 mm outer diameter with a flattened tip (United Sensor, U.S.A., USC-E-120-03). A locally made Preston tube of 1.0 mm outer diameter and 0.6 mm inner diameter was used for shear stress measurements at the wall in the diffuser. A Betz projection manometer of 0.1 mm of water graduation was used for static and Pitot pressure measurements. As suggested by Kovasznay (1966) a Pitot tube made from stainless steel tube of 1 mm outer diameter and 0.6 mm inner diameter, along with a Combist micro-manometer (0.01 mm of water graduation) was used to measure the velocity profile in the sub-layer for a free stream velocity of 4.0 ms^{-1}. The closest point to the wall at which the velocity could be measured with this tube was 0.15 mm.

Hot wire measurements were made with a standard DISA boundary layer probe 55P05 (1.25 mm wire length, 5 μm wire diameter). The electronic equipment included a Constant Temperature Anemometer, DISA 55M10; a Linearizer, DISA 55M25; an R.M.S. Meter, DISA 55D35; a Digital Voltmeter, DISA 55D31; a Turbulence Processor, DISA 52B25; a Dual Beam Storage Scope, Tektronix DM43; and a True Integrator, DISA 52B30. A locally made differentiator, TM-TD-1 (Trimet Instruments) was also used. An OHM-meter was used to indicate contact when the probe touched the wall.

4.0 RESULTS AND DISCUSSION

The basic purpose of this research was to measure the shear stress at the wall in a diffuser with a hote wire probe. Hot wire measurements close to the wall are affected by the heat transfer to the wall, therefore these readings require a correction. The method for correction was developed in a boundary layer flow on the wall of a pipe. This flow was studied for its general characteristics and the data was compared with other peoples' results in boundary layer flow (over a flat plate and on the wall of a pipe) before applying the correction. In the following paragraphs the general characteristics of the boundary layer flow will be discussed. The correction procedure developed in this flow will be described and finally the diffuser flow results will be discussed.

4.1 BOUNDARY LAYER FLOW

The data being produced here were obtained at three free stream velocities of 4.0, 7.5 and 12.0 ms^{-1}. The boundary layer parameters corresponding to these velocities are given in Table I.

Mean velocity and turbulence data show that these flows are representative of a boundary layer as developed on a flat plate.

Figure 2 shows boundary layer mean velocity distributions obtained with a hot wire. (The velocities close to the wall

have been corrected as described later). The velocity distributions in the wall layer and core region intersect around $Y^+ = 15$, which indicates the point of maximum turbulence production (see Figure 4). The three velocity distributions coincide in the turbulent core region. A similar graph has been presented by Repik and Sosedko (1976).

Mean velocity measurements in the boundary layers, obtained with a Pitot tube, are shown in Figure 3, which is a plot of U^+ vs. Y^+. The U^* values used for plotting this graph were obtained from the cross-plot method applied to the Log. Law in the form $U^+ = 5.6 \text{ Log}_{10} Y^+ + 5.0$. The figure shows a region of good agreement of the Log. Law in the boundary layer for these velocities.

The R.M.S. value of the longitudinal fluctuating velocity component divided by friction velocity has been plotted in Figure 4. This graph peaks around $Y^+ = 15$ which indicates maximum turbulence production at this point. The present data has been compared with Ueda and Hinze (1975) and Morrison and Kronauer (1969) and it agrees with their results.

Turbulence intensity and local mean velocity divided by free stream velocity have been plotted against linear distance from the wall in Figure 5. Turbulence intensity peaks around $Y^+ = 5$ which is the edge of the sub-layer (this is one of the characteristics of the sub-layer). The mean

velocity profile similar to the one shown in Figure 2 has an intersection point of tangents drawn to the wall layer and turbulent core region at $Y^+ = 17$ which is close to the point of maximum turbulence production.

The flatness factor of $\partial u/\partial t$ has been plotted against Y^+ in Figure 6 for the boundary layer flow in a pipe and fully developed pipe flow. $F(\partial u/\partial t)$ has very high values in the sub-layer and in the intermittent region of the boundary layer. Frankiel and Klebanoff (1975) and Sabot and Comte-Bellot (1976) have shown that the intermittency of the outer region in the boundary layer begins around $Y/\delta = 0.4$. In the present experiment values of Y^+ of 196, 284 and 500 correspond to $Y/\delta = 0.4$ for free stream velocities of 4.0, 7.5 and 12.0 ms^{-1} respectively. Figure 6 shows that $F(\partial u/\partial t)$ is very high in the sub-layer and decreases away from the wall. It becomes constant (approximately 6) for all the velocities at $Y^+ = 125$ and then increases again at $Y^+ = 180$ for 4.0 ms^{-1}, at $Y^+ = 260$ for 7.5 ms^{-1} and at $Y^+ = 450$ for 12.0 ms^{-1} (in the boundary layer in a pipe) but remains constant (approximately 6) in fully developed pipe flow. These values of Y^+ are close to the calculated values of Y^+ corresponding to $Y/\delta = 0.4$. Therefore it can be concluded that the boundary layer and fully developed pipe flows are similar in the region where $Y/\delta < 0.4$.

Figure 7 shows comparison of skewness of $\partial u/\partial t$ measure-

ments with Ueda and Hinze (1975) and Elena (1977). Skewness factor is an indication of asymmetry of the probability density. It peaks between Y^+ of 10 and 15 and decreases towards the wall which is an indication of the presence of the sub-layer adjacent to the wall. There is more scatter in the wall layer than in the core region mostly due to errors in fine distance measurements and probe positioning. The present results agree quite well with those of Ueda and Hinze, and Elena.

4.2 THE CORRECTION PROCEDURE

The two methods of correcting hot wire measurements very close to the wall were developed in a boundary layer flow in a pipe.

The first method, formulated by Oka and Kostic (1972) and Zemskaya et al. (1979), is based on the existence of the linear velocity law in the sub-layer, $U^+ = Y^+$. Uncorrected hot wire velocity measurements have been plotted in the form of U^+ vs. Y^+ graphs for six free stream velocities ranging from 2.5 to 12.0 ms^{-1} in Figure 8. This plot requires true friction velocity values from some other method such as the Log Law. Figure 9 was developed from Figure 8 by noting the deviation of the measured velocity distribution from the line $U^+ = Y^+$, and plotting it against the corresponding Y^+ on a log log graph. According to Zemskaya et al. (1979) two

straight lines of gradients -1 and -2 are obtained from this graph. These lines have been shown in Figure 9. The position of Y^+, where these two lines intersect, corresponds to the mean minimum position of the uncorrected velocities of Figure 8. (No minima are available for 10.0 and 12.0 ms^{-1}). Its value (designated by Y^+_{unc}) is noted for future use. This position is the same for all the free stream velocities. Then uncorrected measured velocities, $\bar{U}_{unc}$, are plotted against distance Y (Figure 10) and Y_{unc} corresponding to the minimum position in these curves is noted. There are minima for $U_\infty \leq 7.5$ ms^{-1} but not for 10 and 12 ms^{-1} because the minimum position gets closer to the wall as the free stream velocity increases. In the present measurements no minima could be obtained for 10 and 12 ms^{-1}, therefore, the friction velocity for these two velocities could not be calculated. Now Y^+_{unc} and Y_{unc} are known. Therefore U^* can be calculated:

$$Y^+_{unc} = \frac{Y_{unc} \times U^*}{\nu} ,$$

or

$$U^* = \frac{Y^+_{unc} \times \nu}{Y_{unc}} .$$

The corrected U^* values have been listed in Table II. The value of Y^+_{unc} is not universal as has been claimed by Zemskaya et al. (1979). In their case Y^+_{unc} is 2.06, Oka

& Kostic (1972) get it as 1.9 and in the present case it is 1.3.

This method was used to check the claim of Zemskaya et al. about the universality of the minimum Y^+_{unc} position. According to their opinion, Y^+_{unc} is the same for all free stream velocities; then only uncorrected velocity measurements are required for calculating the friction velocity, i.e., if Y_{unc} is known for a particular free stream velocity the U^* can be obtained from

$$U^* = \frac{Y^+_{unc}\,\nu}{Y_{unc}} \quad .$$

But Y^+_{unc} did not turn out to be universal. Also this method requires measurements close enough to the wall so that the minimum value of $\bar{U}_{unc}$ can be located. This will require a hote wire probe of tips finer than the DISA 55P05 boundary layer type of probe, a locally flat surface, and a very accurate distance measurement (of the order of a micron).

The second method, which was later applied in the diffuser flow measurements consisted of using a boundary layer type of probe, adjusting the linearizer, and traversing the probe in the wall region with and without flow. An electric circuit was used to indicate when the probe was just touching the wall. The hot wire voltage at each location from the wall for each condition was noted. The

true velocity was obtained by subtracting the no flow voltage from the flow voltage. The results are presented dimensionally in Figure 11 using a linear scale. The velocity gradients were measured from the corrected velocity profiles in Figure 11 for calculating the friction velocity for different free stream velocities. The friction velocities thus obtained were then used to plot the corrected velocity profiles non-dimensionally in the form U^+ vs. Y^+ in Figure 12 using a log-linear scale. It is interesting to note in Figure 12 that the corrected points are following the $U^+ = Y^+$ curve upto $Y^+ = 5$ (approximately). This shows the validity of this correction. The friction velocity values obtained by this method have been listed in Table II and compared with other peoples' boundary layer results in the present experimental range of free stream velocities (Figure 13).

Since Pitot tube measurements do not require a correction for wall heat loss, a flattened tip Pitot tube along with a Combist Micro-manometer was used for measuring the velocity profile in the sub-layer for a free stream velocity of 4.0 ms^{-1}. The friction velocity so obtained has been listed in Table II. The closest point to the wall at which the velocity could be measured with this tube was 0.15 mm. The approximate sub-layer thicknesses (corresponding to $Y^+ = 5$) for 4.0, 7.5 and 12.0 ms^{-1} are 0.45, 0.28 and 0.16 mm respectively. The sub-layer is quite thick for 4.0 ms^{-1}. For 7.5 ms^{-1} it is

difficult to measure the velocity satisfactorily at several points between 0.15 & 0.28 mm due to such difficulties as errors in measuring very small distances, difficulty in measuring the very small magnitude of pressure with the micro-manometer, and the aerodynamic effect.

4.3 DIFFUSER FLOW

The pipe flow entering the diffuser was fully developed. Nikuradse (1926) suggested a minimum length/diameter of 40 for pipe flow to become fully developed, for practical purposes whereas Laufer (1954) showed that a ratio of 50 is better. In the present setup a ratio of 73 has been used. The average velocity was measured at a quarter radius from the pipe wall. By integrating the velocity profile, it was confirmed that the bulk mean velocity is closely recorded at the quarter radius position. The ratio of mean bulk velocity to maximum velocity was found to be 0.84 at the reference station at Re_{av} = 117,000. According to the power law, $\frac{\bar{U}}{U_{cL}} = (\frac{Y}{R})^n$, the value of the index n equal to 1/8 fits the experimental results well for Re_{av}, between about 100,000 and 400,000, and the corresponding U_{av}/U_{cl} is equal to 0.84 at quarter radius (Schlichting 1968). This agrees with the present results.

Figure 1 shows the diffuser geometry. Sprenger (1959) and Sovran, and Klomp (1967) found that this kind of diffuser possesses optimum pressure recovery characteristic.

The static pressure distribution and static pressure derivative along the length of the diffuser is shown in Figure 14. The non-dimensional static pressure collapses for the three Re_{av} values of 117,000, 83,000 and 68,000 which shows that the flow is similar at these Reynolds numbers. It may be expected since the flow entering the diffuser is fully developed.

An axisymmetric line was located in the diffuser flow by Okwuobi and Azad (1973) along which the turbulence intensity is maximum and S(u) = 0. In the present experiment this line was established by marking the distance of the points from the wall where S(u) was zero and u' reached its peak value at several stations along the wall of the diffuser. It has been shown in Figure 13. This line may be called the E_p (Energy Peak) line for distinction. Mean velocity measurements along this line (Figure 15) show that the mean velocity remains constant along this line.

Skewness and flatness of $\partial u/\partial t$ are plotted against Y^+ in Figure 16 at 12 cm upstream from the exit of the diffuser. The measurements were made at 12 cm upstream from the exit of the diffuser from the wall to the centreline. This is a very interesting plot. It shows the presence of the sub-layer in the diffuser flow because $S(\partial u/\partial t)$ increases from the wall upto $Y^+ = 10$ and then decreases as was observed in the boundary layer flow. $S(\partial u/\partial t)$ finally becomes constant

(approximately 0.4) between the energy peak line and the centreline. This fact shows that the diffuser flow could be considered locally isotropic between the energy peak line and the centreline. The present results agree with Arora & Azad's results (1980). Sub-layer measurements were not made by Arora & Azad. The flatness of $\partial u/\partial t$ has very high values close to the wall and decreases away from the wall. It becomes constant between the energy peak line and the centreline, which again proves that the diffuser flow is locally isotropic in this region.

Figure 17 is a plot of negative skewness of $\partial u/\partial t$ vs. flatness of $\partial u/\partial t$ at 12 cm upstream from the exit of the diffuser at Re_{av} = 117,000. The straight line represents the equation $-S\left(\frac{\partial u}{\partial t}\right) = 0.23\left[F\left(\frac{\partial u}{\partial t}\right)\right]^{0.362}$ obtained by Van Atta and Antonia (1980) on the basis of data obtained by many experimentalists. It is interesting to note that those experiments were done in flows in the atmosphere, pipes, wakes, jets and two dimensional ducts. The present result is in diffuser flow.

Basically two methods were used for measuring the shear stress at the wall in the diffuser flow. The first method was to determine the slope, at the wall, of the velocity profile obtained from the direct hot wire measurements with correction for wall effect. The second method was through pressure measurements with a Preston tube using Patel's calibration which is applicable in adverse pressure

gradient if $(U^* d)/\nu \leq 250$.

The hot wire was used to measure the velocity gradient at the wall at several stations along the length of the diffuser. The second method of correcting the hot wire measurements was applied here. The corrected friction velocity values have been plotted in Figure 18. Hot wire measurements could not be done all along the length of the diffuser due to difficulties in precisely positioning the probe at the wall more than 35 cm ahead of the exit of the diffuser.

A Preston tube was made from 1.0 mm outer diameter and 0.6 mm inner diameter stainless steel tube. The pressure difference ΔP between the Preston tube and static hole was measured while the Preston tube was lying at the wall at several stations along the diffuser and pipe. The pressure difference was then used to calculate the friction velocity from Patel's calibration (1965). The friction velocity so obtained was corrected by Frei and Thomann's method. They developed this method by measuring skin friction in an adverse pressure gradient using a sealed floating element technique. This is a very accurate method because direct measurement of the force on the floating element is done with Piezo-electric transducers with high sensitivity. This apparatus was mainly used to investigate the error of Preston tubes in adverse pressure gradients. The corrected friction

velocity measurements show excellent agreement with the hot wire measurements.

5.0 CONCLUDING REMARKS

In a turbulent boundary layer flow, very close to the wall, a linear velocity profile exists with the boundary condition of zero velocity at the wall. In this flow the criterion for judging the accuracy of the correction to hot wire measurements for wall effects is that the corrected velocity profile should be $\bar{U} = Y \times \text{constant}$ or $U^+ = Y^+$. The results obtained by applying Van Der Hegge Zijnen's method of wall correction to hot wire measurements in the boundary layer flow satisfy the above mentioned criterion very well and the method is judged to be satisfactory.

The measurements of mean velocity, turbulence intensity, skewness of $\partial u/\partial t$ and flatness of $\partial u/\partial t$ in the boundary layer in a pipe and comparison with the available data in the boundary layer over flat plates and in pipes shows that the sub-layer has the following characteristics:

(a) A linear velocity profile exists with zero velocity at the wall.

(b) The local turbulence intensity, $u'/\bar{U}$, reaches a maximum value at the outer edge of the sub-layer ($Y^+ = 5$).

(c) Skewness of $\partial u/\partial t$ in this layer decreases towards the wall.

(d) Flatness of $\partial u/\partial t$ increases towards the wall.

(e) The boundary layer flows are similar in the wall region whether the boundary layer is developed over a flat plate or in a pipe.

The measurements in the diffuser flow show that a sub-layer also exists in this flow. The friction velocity measured with a hot wire and the Preston tube along the wall of a pipe and the attached diffuser remains constant in the fully developed pipe flow, decreases sharply in the first half of the diffuser and then decreases linearly in the second half of the diffuser. The mean velocity remains constant along the energy peak line in this flow.

The shear stress at the wall can be measured by three methods, namely, cross-plot method using the Log. Law, the Preston tube using Patel's calibration, and the wall velocity profile obtained by the hot wire. There are certain limitations to the use of these methods. The cross-plot method can only be used if the Log. Law is applicable in the flow, the Preston tube cannot be used if $U^{*}d/\nu > 250$, and the hot wire measurements require a correction in the proximity of the wall. The first two methods are easier to handle; the hot wire needs lot of care and precautions. In an adverse pressure gradient (diffuser flow), where the Log Law is not applicable (over a range long enough to ensure the validity of cross-plot method), the Preston tube can be satisfactorily used for shear stress measurements at the wall.

6.0 REFERENCES

1. Arora, S.C. and Azad, R.S. 1980, "Applicability of the Isotropic Vorticity Theory to an Adverse Pressure Gradient Flow", J. Fluid Mech., Vol. 97, Part 2.

2. Azad, R.S. and Hummel, R. 1971, "Measurement of the Intermittency Factor in Diffuser Flow", Canadian Journal of Physics, Vol. 49, No. 23.

3. Chauve, Marie-Pierre. 1977, "Determination Directe Due Frottement Sur Une Paroi Poreuse A L'Aide D'Un Anemometre", Colloque Euromech 90, Nancy, 4-8 Juillet.

4. Clauser, F.H. 1956, "The Turbulent Boundary Layer", Adv. Appl. Mech., Vol. 4, N.Y.

5. Coles, D. 1955, "The Law of the Wall in Turbulent Shear Flow", 50 Jahre Grenzschichtforschung, Vieweg, Braunschweig.

6. Comte-Bellot, G. 1965, "Ecoulement Turbulent Entre Deux Parois Paralleles, Publ. Sci. Tech. Min. Air, No. 419, Paris.

7. Dryden, H.L. 1936, "Air Flow in the Boundary Layer Near a Plate", NACA Tech. Rep. No. 562.

8. Elena, M. 1977, "Etude Des Structures Dynamiques et Thermiques D' Un Ecoulement Turbulent en Conduite Avec Aspiration a La Pardi", Division De Chimie, Centre D' Etudes Nucleaires De Saclay, Rapport CEA-R-4843.

9. Frei, D. and Thomann, H. 1980, "Direct Measurements of Skin Friction in a Turbulent Boundary Layer with a Strong Adverse Pressure Gradient", Private Correspondence.

10. Frankiel, F.N. and Klebanoff, P.S. 1975, "On the Lognormality of the Small Scale Structure of Turbulence", Boundary Layer Meteorology 8.

11. Hegge Zijnen, B.G. Van Der. 1924, "Measurements of the Velocity Distribution in the Boundary Layer Along a Plane Surface", Thesis, Delft.

12. Hinze, J.O. 1962, "Turbulent Pipe Flow", International Symposium of the National Scientific Research Centre (CNRS), The Mechanics of Turbulence, Marseille, August 28th to September 2nd, Gordon and Breach Science Publishers.

13. Kibens, V. 1968, "The Intermittent Region of a Turbulent Boundary Layer", Ph.D. Thesis, The Johns Hopkins University, Baltimore, Maryland, U.S.A.

14. Klebanoff, P.S. and Diehl, Z.W. 1952, "Some Features of Artificially Thickened Fully Developed Turbulent Boundary Layers with Zero Pressure Gradient", NACA Report No. 1110.

15. Kovasznay, L.S.G. 1966, "Turbulence Measurement", Applied Mechanics Survey, Edited by H.N. Abramson et al., MacMillan and Co.

16. Landau, L.D. and Levich, V.G. 1959, "Fluid Mechanics", Pergamon Press, London.

17. Laufer, J. 1954, "The Structure of Turbulence in Fully Developed Pipe Flow", NACA Report No. 1174.

18. Levich, V.G. 1962, "Physiochemical Hydrodynamics", Prentice Hall Inc., U.S.A.

19. Morrison, W.R.B. and Kronauer, R.E. 1969, "Structural Similarity for Fully Developed Turbulence in Smooth Tubes", J. Fluid Mech., Vol. 39, Part 1.

20. Nikuradse, J. 1929, "Untersuchungen Uber Die Stromungen Des Wassers in Konvergenten Und Divergenten. Kanalen", Forsch. Geb. Ing. Wes., Heft 289.

21. Oka, S. and Kostic, Z. 1972, "Influence of Wall Proximity on Hot Wire Velocity Measurements", DISA Electronik, Skovlunde Denmark, Information No. 13.

22. Okwuobi, P.A.C. and Azad, R.S. 1973, "Turbulence in a Conical Diffuser with Fully Developed Flow at Entry", J. Fluid Mech., Vol. 57, Part 3.

23. Patel, V.C. 1965, "Calibration of the Preston Tube and Limitations on its Use in Pressure Gradients", J. Fluid Mech., Vol. 23, Part 1.

24. Prandtl, L. 1952, "Essentials of Fluid Dynamics", Blackie, London.

25. Reichardt, H. 1940, "Die Warmeubertragung in Turbulenten Reibungschichten", Zeit Ang. Math. Mech. 20, 297.

26. Repik, Ye. U. and Sosedko, Yu. P. 1976, "Investigation of the Discontinuous Flow Structure in the Wall Region of a Turbulent Boundary Layer", Fluid Mechanics - Soviet Research, Vol. 5, No. 6.

27. Sabot, J. and Comte-Bellot G. 1976, "Intermittency of Coherent Structures in the Core Region of Fully Developed Turbulent Pipe Flow", J. Fluid Mech., Vol. 74, Part 4.

28. Schlichting, J. 1968, "Boundary Layer Theory", 6th Ed., McGraw-Hill, New York.

29. Sovran, G. and Klomp, E.D. 1967, "Experimentally Determined Optimum Geometries for Rectilinear Diffusers with Rectangular, Conical or Annular Cross-Section", General Motors Symposium on Internal Flow, Elsevier Publishing Co., Amsterdam.

30. Sprenger, H. 1959, "Experimentelle Untersuchungen an Geraden Und Gekrummten Diffusoren Mitt. Inst. Aerodyn., Zurich, (English Translation: - Rep. TIL/T5134, Technical Information and Library Services, The British Ministry of Aviation).

31. Townsend, A.A. 1956, "The Structure of Turbulent Shear Flow", Cambridge University Press.

32. Trupp, A.C. 1973, "The Structure of Turbulent Flow in Triangular Array Rod Bundles", Ph.D. Thesis, Dept. of Mech. Eng., The University of Manitoba.

33. Ueda, H. and Hinze, J.O. 1975, "Fine Structure Turbulence in the Wall Region of a Turbulent Boundary Layer", J. Fluid Mech., Vol. 67, Part 1.

34. Van Atta, C.W. and Antonia, R.A. 1980, "Reynolds Number Dependence of Skewness and Flatness Factors of Turbulent Velocity Derivatives", The Physics of Fluids, Vol. 23, No. 2.

35. Weissberg, H.L. 1956, "Velocity Profiles and Friction Factors for Turbulent Pipe Flow with Uniform Wall Suction", Physics Rep. K, 1264, Oak Ridge, Tennessee.

36. Wills, J.A.B. 1962, "The Correction of Hot Wire Readings for Proximity to a Solid Boundary", J. Fluid Mech., Vol. 12, Part 3.

37. Zemskaya, A.S., Levitskiy, V.N., Repik, Ye. U. and Sosedko, Yu. P. 1979, "Effect of the Proximity of The Wall on Hot Wire Readings in Laminar and Turbulent Boundary Layers", Fluid Mechanics - Soviet Research, Vol. 8, No. 1.

APPENDIX

The boundary layer thickness, displacement thickness, momentum thickness, skewness factor and flatness factor are defined here.

Boundary Layer Thickness, δ:

In a flow over a flat plate the fluid velocity at the plate is zero and it increases assymptotically to the free stream velocity at the outer edge of the boundary layer. Because the outer edge is not distinct, it is convenient to denote the thickness of the boundary layer as the distance in which the fluid velocity is less than 0.99 U_∞. There is generally some ambiguity in speaking of the boundary layer "thickness" if what is meant is the region in which the velocity changes from U_∞ to zero. It is found both convenient and more useful to define some boundary layer thickness parameters that are unambiguous. These are called the displacement thickness and the momentum thickness.

Displacement Thickness δ_1:

The displacement thickness is a measure of the displacement of the main stream resulting from the presence of slow moving fluid in the boundary layer. It is the thickness of a zero velocity layer that has the same mass flow deficit as the actual boundary layer.

Let δ_1 be the displacement thickness considering incompressible axisymmetric flow,

The loss of volume flow = $\int_{R-\delta}^{R} (U_\infty - \bar{U}) 2\pi r dr = A_1 U_\infty$,

where $A_1 = [\pi R^2 - \pi(R - \delta_1)^2]$.

Therefore

$$U_\infty[\pi R^2 - \pi(R - \delta_1)^2] = \int_{R-\delta}^{R} (U_\infty - \bar{U})\, 2\pi r dr$$

$$2R\delta_1 - \delta_1 = \int_{R-\delta}^{R} (1 - \frac{\bar{U}}{U_\infty})\, d\,(r^2) \ .$$

Let $X_d = \int_{R-\delta}^{R} (1 - \frac{\bar{U}}{U_\infty})\, d(r^2)$,

Then

$$\delta_1^2 - 2R\delta_1 + X_d = 0 \ ,$$

$$\delta_1 = R - \sqrt{R^2 - X_d} \ , \text{ (negative root only).}$$

For obtaining the displacement thickness, the velocity profile measurements in the boundary layer were plotted in the form $(1 - \frac{\bar{U}}{U_\infty})$ vs r^2, where r varied from R to $(R - \delta)$ and the integral X_d was calculated by measuring the area, with a planimeter, under the above-mentioned graph. The displace-

ment thickness measurements have been listed in Table I.

Momentum Thickness δ_2:

The momentum thickness is a measure of the momentum flux decrement caused by the presence of the boundary layer. It is the thickness of a zero velocity layer that has the same momentum flux deficit as the actual boundary layer.

Let δ_2 be the momentum thickness. Considering incompressible axisymmetric flow,

$$\text{The loss of momentum flux} = \int_{R-\delta}^{R} \rho\bar{U}(U_\infty - \bar{U})\, 2\pi r dr$$

$$= \rho A_2 U_\infty^2 ,$$

where $A_2 = [\pi R^2 - \pi(R - \delta_2)^2]$.

Therefore

$$U_\infty^2 [\pi R^2 - \pi(R - \delta_2)^2] = \int_{R-\delta}^{R} \bar{U}(U_\infty - \bar{U})\, 2\pi r dr$$

$$2R\delta_2 - \delta_2^2 = \int_{R-\delta}^{R} \frac{\bar{U}}{U_\infty}\left(1 - \frac{\bar{U}}{U_\infty}\right) d(r^2) .$$

$$\text{Let } X_m = \int_{R-\delta}^{R} \frac{\bar{U}}{U_\infty}\left(1 - \frac{\bar{U}}{U_\infty}\right) d(r^2) .$$

Then

$$\delta_2^2 - 2R\delta_2 + X_m = 0 \quad ,$$

$$\delta_2 = R - \sqrt{R^2 - X_m} \quad .$$

The integral X_m was calculated by plotting the velocity profile measurements in the boundary layer in the form $\frac{\bar{U}}{U_\infty}\left(1 - \frac{\bar{U}}{U_\infty}\right)$ vs. r^2 , where r varies from R to $(R - \delta)$, and measuring the area under the curve with a planimeter. The momentum thickness measurements have been listed in Table I.

Skewness and Flatness Factors:

Let $\tilde{u}(t)$ be the instantaneous fluctuating velocity. It is desired to find the relative amount of time that $\tilde{u}(t)$ spends between two adjacent levels. This can be obtained by the use of a gating circuit, which turns on when the signal $\tilde{u}(t)$ is between the two levels. The average output of the gating circuit is proportional to the difference between the two levels, $\Delta\tilde{u}$, so that it is convenient to define a quantity, $B(\tilde{u})$, by

$$B(\tilde{u}) \quad \Delta\tilde{u} = \lim_{T\to\infty} \frac{1}{T} \quad \Sigma \ (\Delta t),$$

where Δt is the interval of time that $\tilde{u}(t)$ spend in $\Delta\tilde{u}$. The function $B(\tilde{u})$ is called the probability density; the probability of finding $\tilde{u}(t)$ between $\tilde{u}$ and $(\tilde{u} + \Delta u)$ is equal

to the proportion of time spent there. The sum of the values of $B(\tilde{u})$ for all $\tilde{u}$ must be equal to 1:

$$B(\tilde{u}) \geq 0 \ , \quad \int_{-\infty}^{\infty} B(\tilde{u})d\tilde{u} = 1 \quad .$$

The mean values of the various powers of $\tilde{u}$ are called moments. The first moment is the familiar mean value, which is defined by

$$\bar{U} = \int_{-\infty}^{\infty} \tilde{u}\, B(\tilde{u})d\tilde{u} \quad .$$

In experimental work, the mean value is always subtracted from the fluctuating function $\tilde{u}(t)$. The fluctuation is denoted by u, so that $u = \tilde{U} - \bar{U}$ and $\bar{u} = 0$. Now $B(\tilde{u}) = B(\bar{U} + u)$, so that it is convenient to use a probability density $B(u)$, which is obtained by shifting $B(\tilde{u})$ over a distance $\bar{U}$ along the $\tilde{U}$ axis. The moments formed with u^n and $B(u)$ are called central moments. The first central moment, of course, is zero. The mean-square departure from the mean value $\bar{U}$ is called the variance, or second moment

$$\overline{u^2} = \int_{-\infty}^{\infty} u^2\, B(u)du \ .$$

The square root of the variance is called standard deviation or R.M.S. amplitude

so $\sqrt{\bar{u}^2} = u' \quad . \ .$

The third moment is defined by,

$$\overline{u^3} = \int_{\infty}^{\infty} u^3 \, B(u) du \ .$$

It depends on the lack of symmetry in B(u). If B(u) is symmetric about the origin, $\overline{u^3} = 0$. It is customary to non-dimensionalize $\overline{u^3}$ by $(u')^3$ or $(\overline{u^2})^{3/2}$, which gives a dimensionless measure of the asymmetry. This is called the skewness (S):

$$S(u) = \frac{\overline{u^3}}{(u')^3} \ .$$

The fourth moment, non-dimensionalized by $(u')^4$ or $(\overline{u^2})^2$ is called the flatness factor (F):

$$F(u) = \frac{\overline{u^4}}{(u')^4} \ .$$

If information about the fine-scale structure is desired then the longitudinal fluctuating velocity u is differentiated with respect to time and skewness and flatness of the differentiated signal $(\partial u/\partial t)$ is measured:

$$S(\partial u/\partial t) = \frac{\overline{(\partial u/\partial t)^3}}{[\overline{(\partial u/\partial t)^2}]^{3/2}} ,$$

and

$$F(\partial u/\partial t) = \frac{\overline{(\partial u/\partial t)^4}}{[\overline{(\partial u/\partial t)^2}]^2} .$$

TABLE I

MEAN QUANTITIES OF THE BOUNDARY LAYER

Free Stream Velocity, U_∞ ms^{-1}	Boundary Layer Thickness, δ mm	Displacement Thickness, δ_1 mm	Momentum Thickness, δ_2 mm	Shape Factor, $H = \frac{\delta_1}{\delta_2}$	$Re_\delta = \frac{U_\infty \delta}{\nu}$	$Re_{\delta_1} = \frac{U_\infty \delta_1}{\nu}$	$Re_{\delta_2} = \frac{U_\infty \delta_2}{\nu}$	$C_f = 2\left[\frac{U^*}{U_\infty}\right]^2$
12.0	46.5	6.41	4.75	1.35	34,880	4,810	3,562	2.94×10^{-3}
7.5	47.5	6.68	4.8	1.39	22,270	3,130	2,250	2.78×10^{-3}
4.0	48.5	6.70	4.95	1.36	12,130	1,680	1,237	3.2×10^{-3}

TABLE II

FRICTION VELOCITY MEASUREMENTS IN BOUNDARY LAYER FLOW

Free Stream Velocity, U_∞ ms^{-1}	Correction Method I (Zemskaya et al.) U^* ms^{-1}	Correction Method II U^* ms^{-1}	Log. Law U^* ms^{-1}	Pitot Tube U^* ms^{-1}
12.0	-	0.42	0.47	-
7.5	0.27	0.27	0.30	-
4.0	0.15	0.14	0.17	0.16

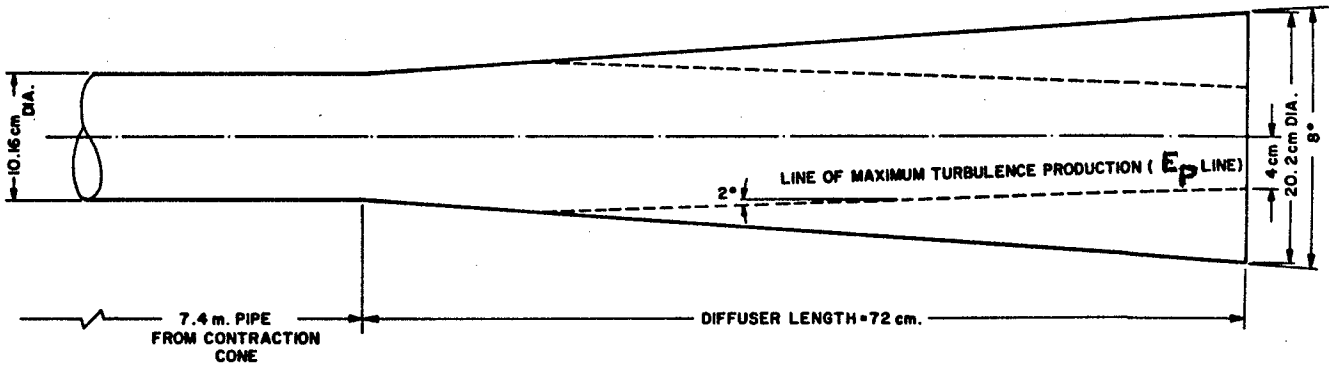

Figure 1. Diffuser geometry.

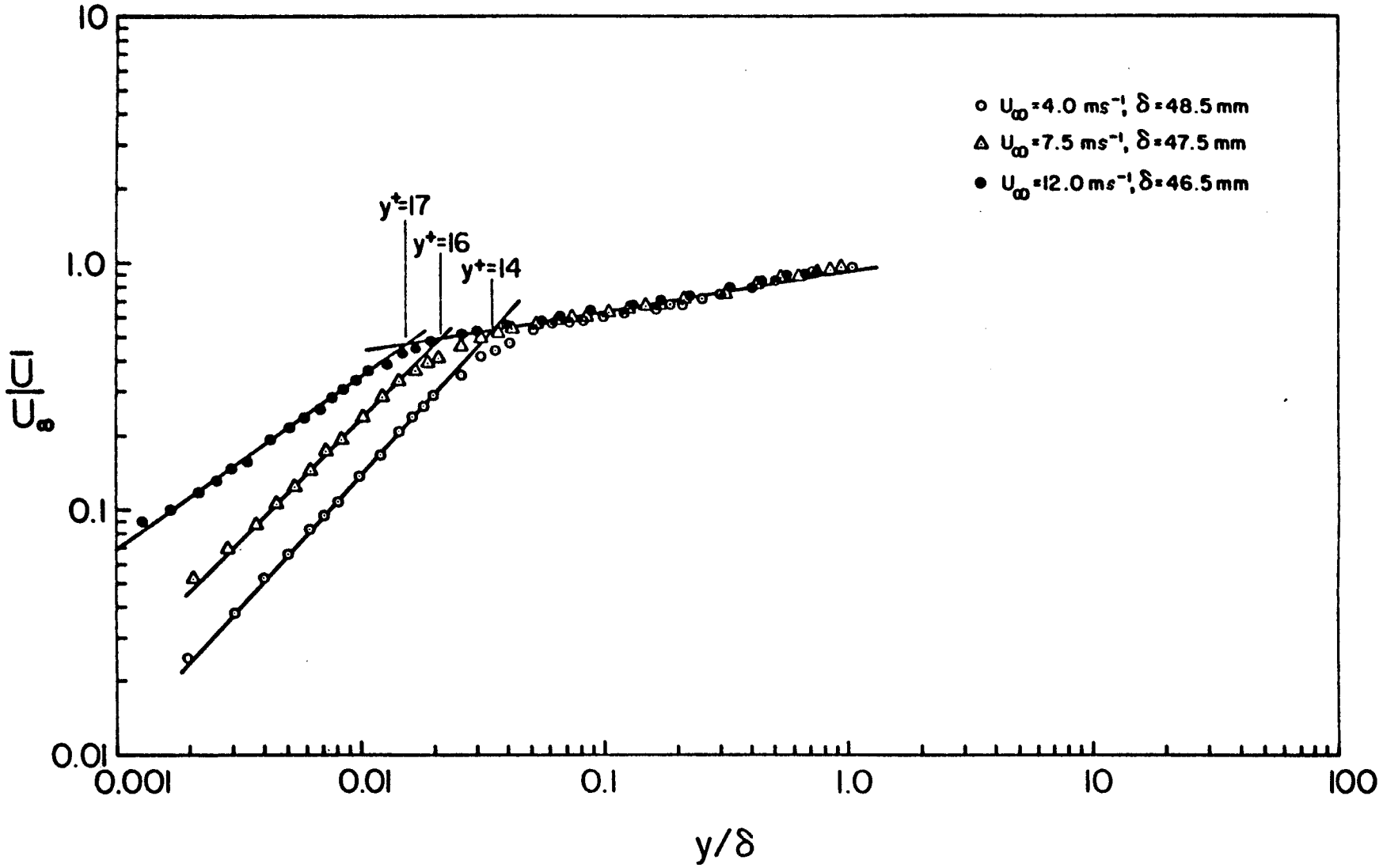

Figure 2. Corrected mean velocity profile in boundary layer.

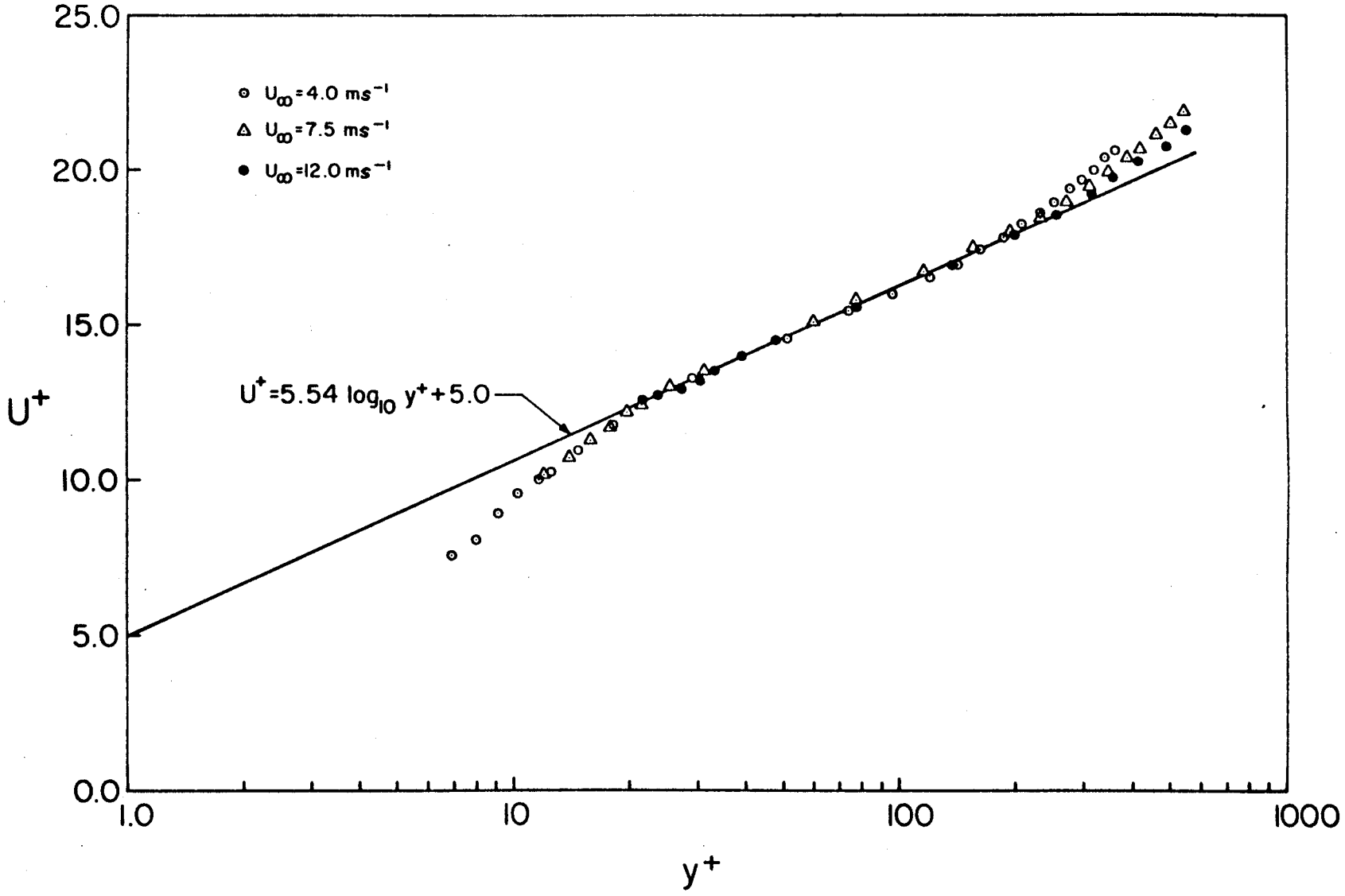

Figure 3. U^+ vs. Y^+ plot obtained with Pitot and Static tubes.

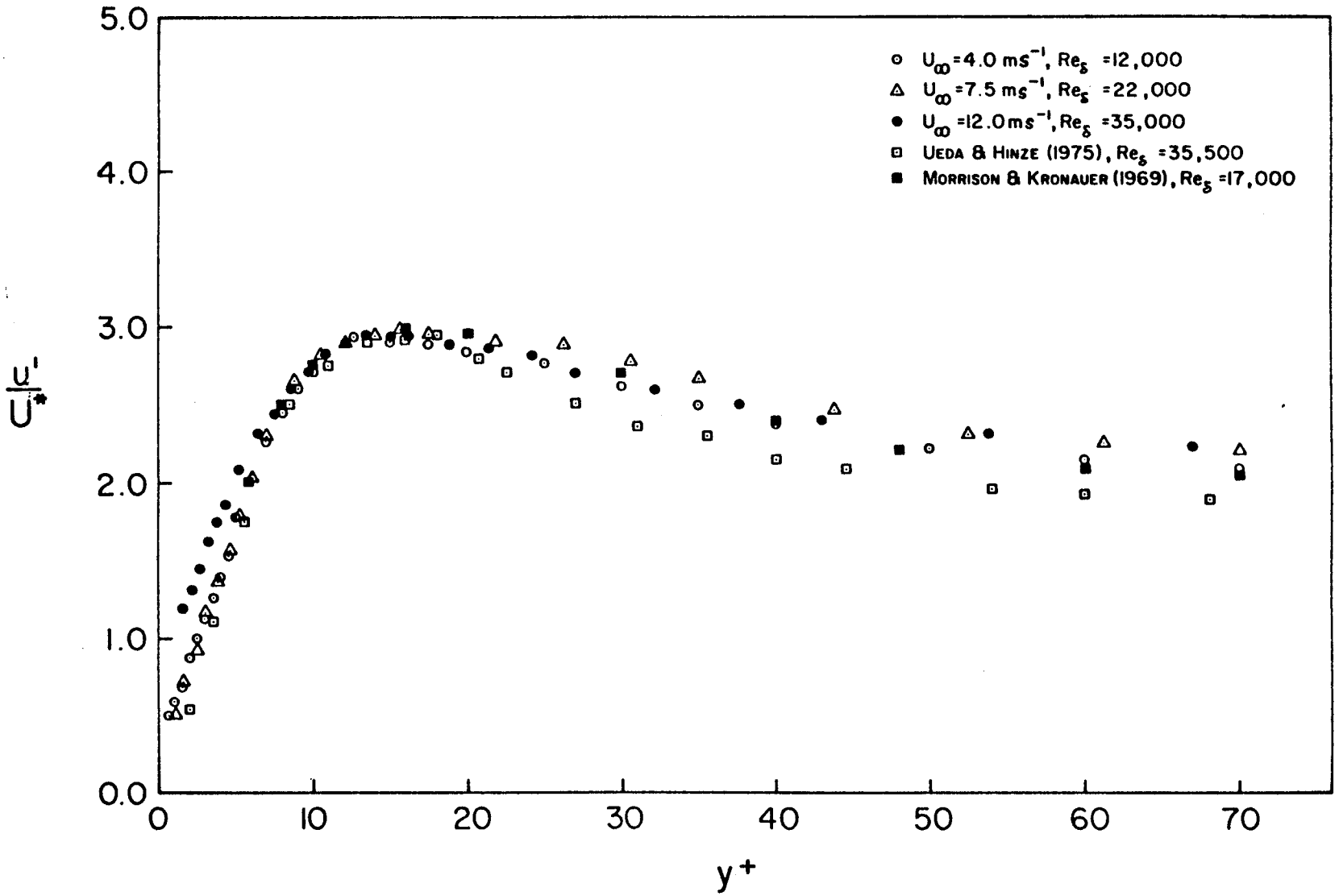

Figure 4. Distribution of longitudinal component of turbulence fluctuations in boundary layer.

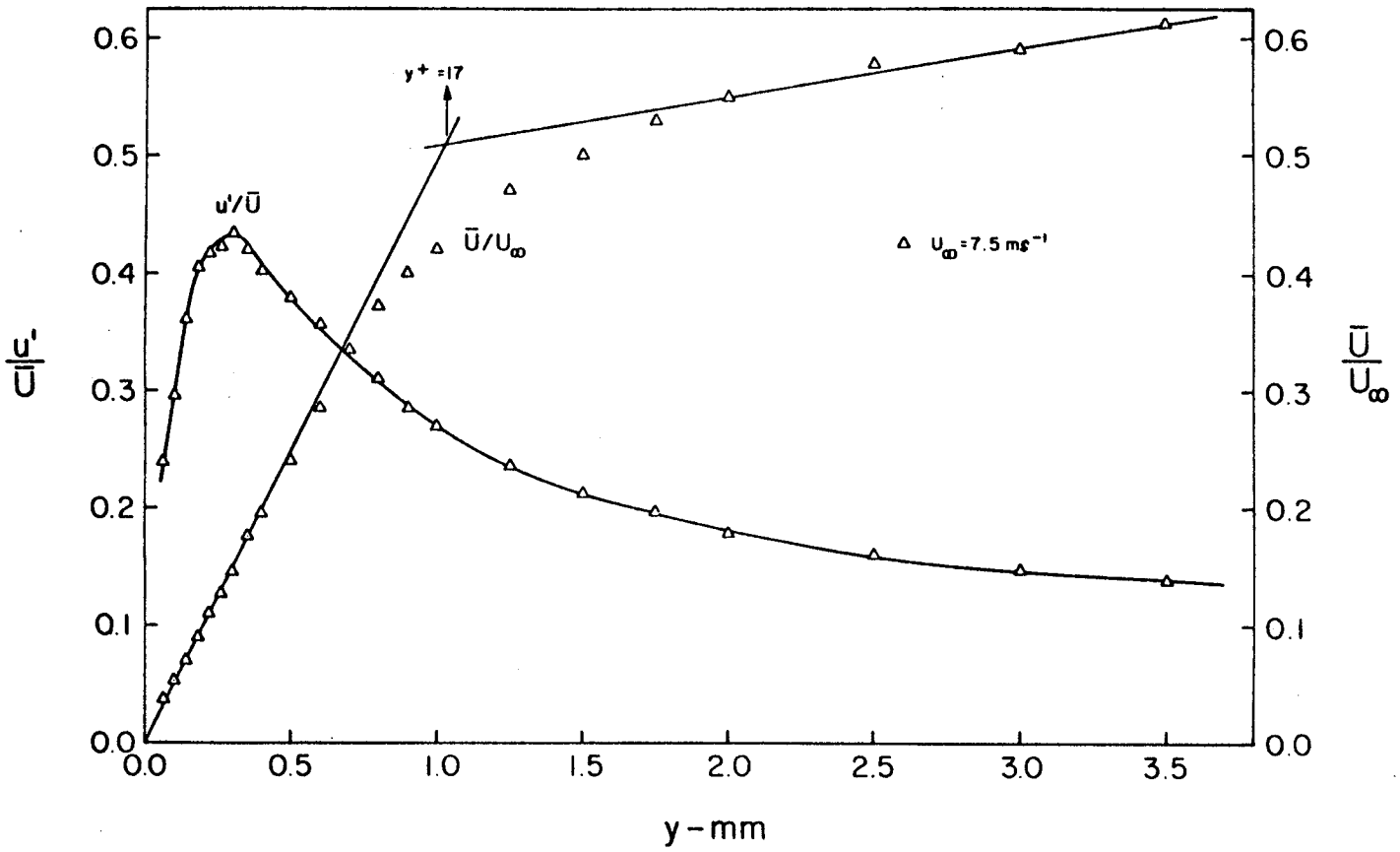

Figure 5. Distribution of turbulence intensity and mean velocity in boundary layer.

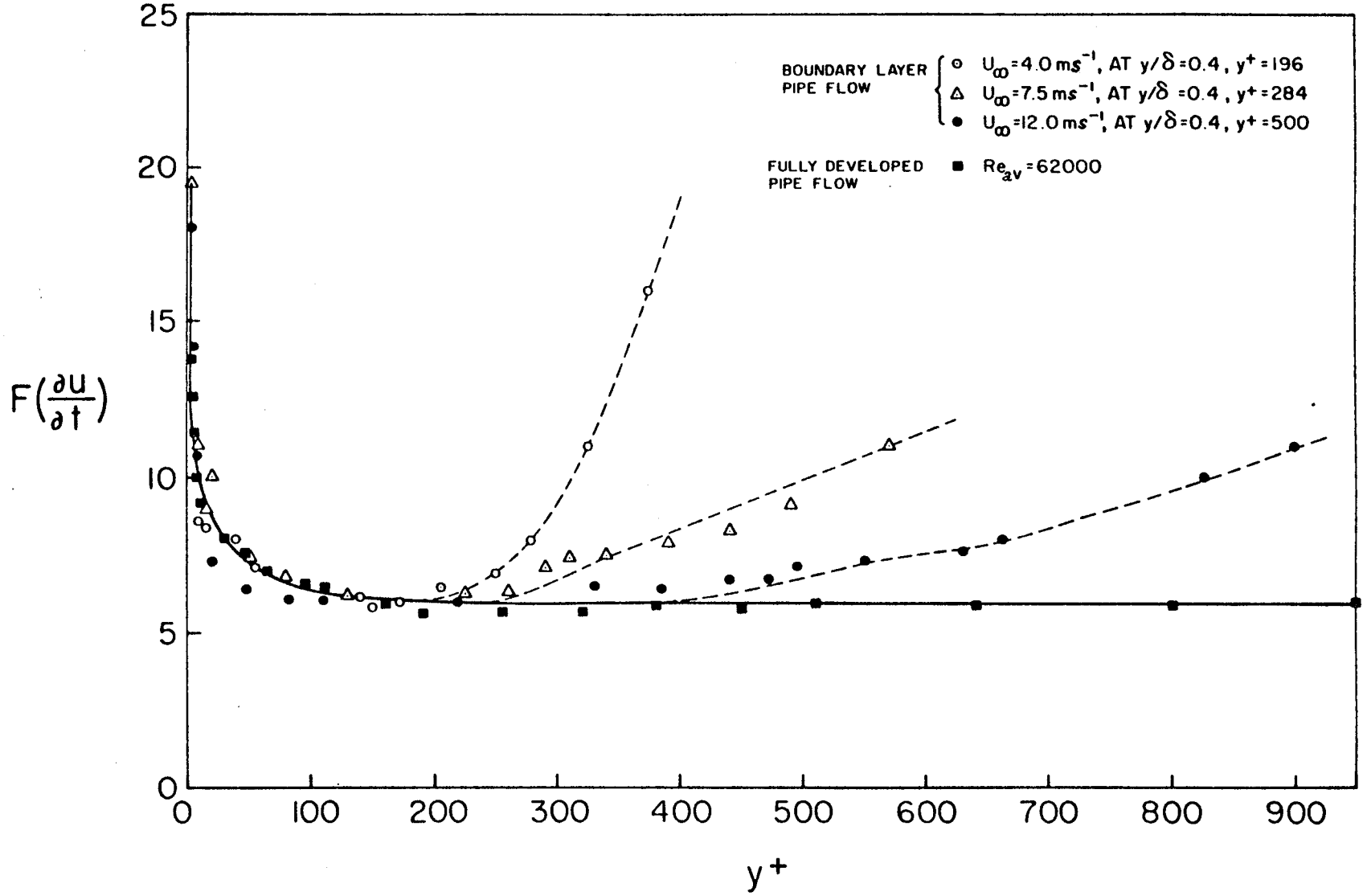

Figure 6. Flatness factor of $\frac{\partial u}{\partial t}$ in boundary layer and fully developed pipe flow.

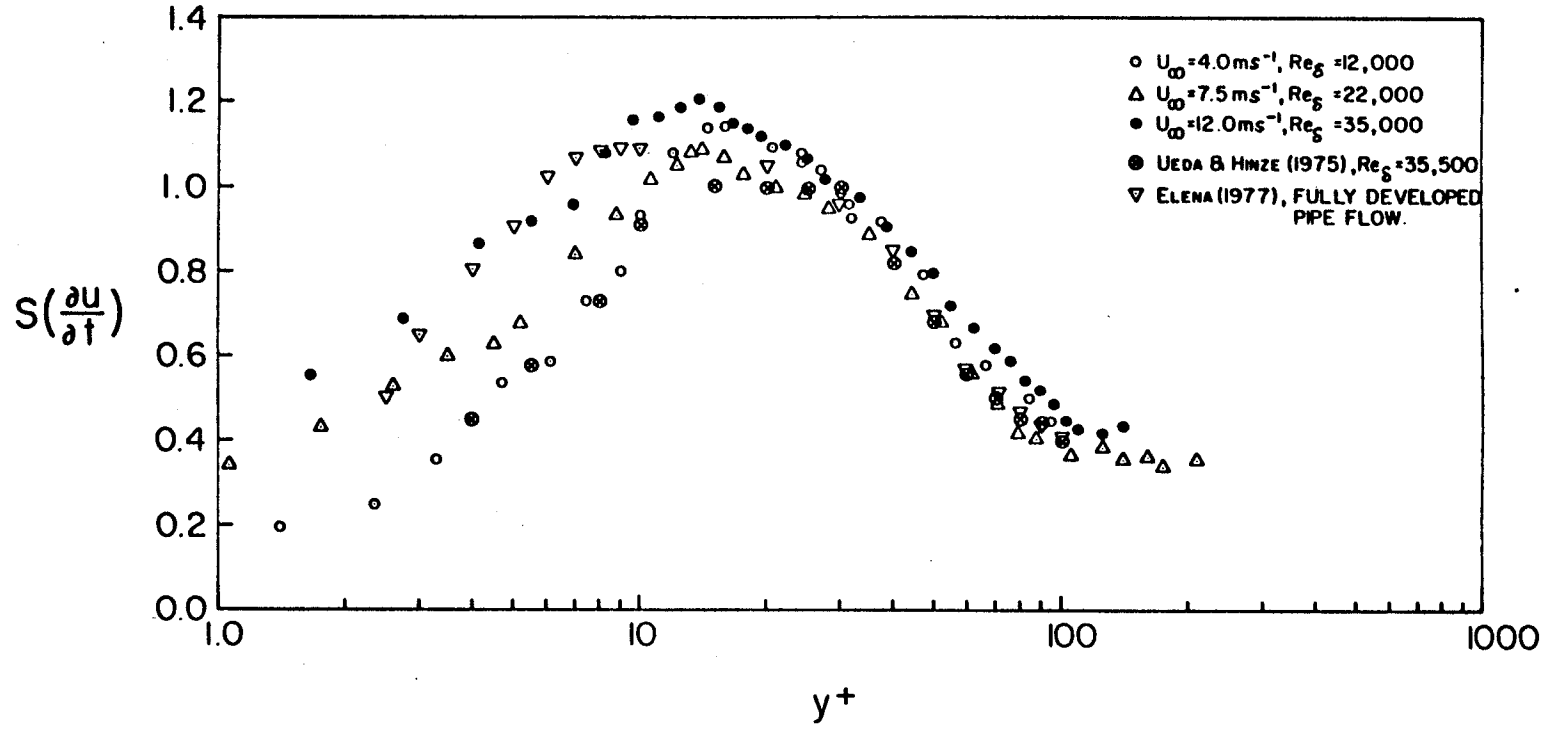

Figure 7. Skewness of $\frac{\partial u}{\partial t}$ in boundary layer and fully developed pipe flow.

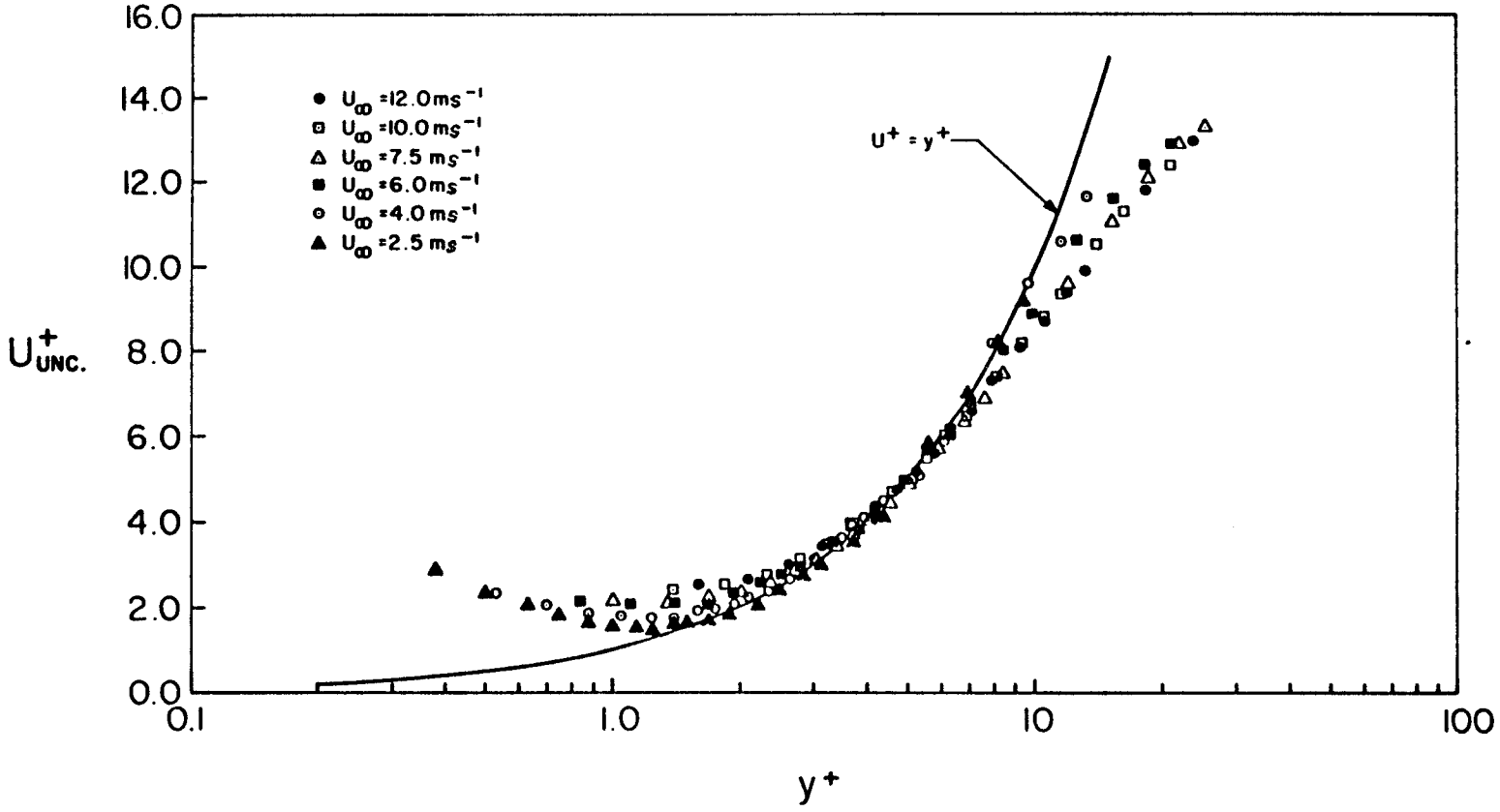

Figure 8. U^+_{unc} vs. Y^+ plot in the proximity of the wall.

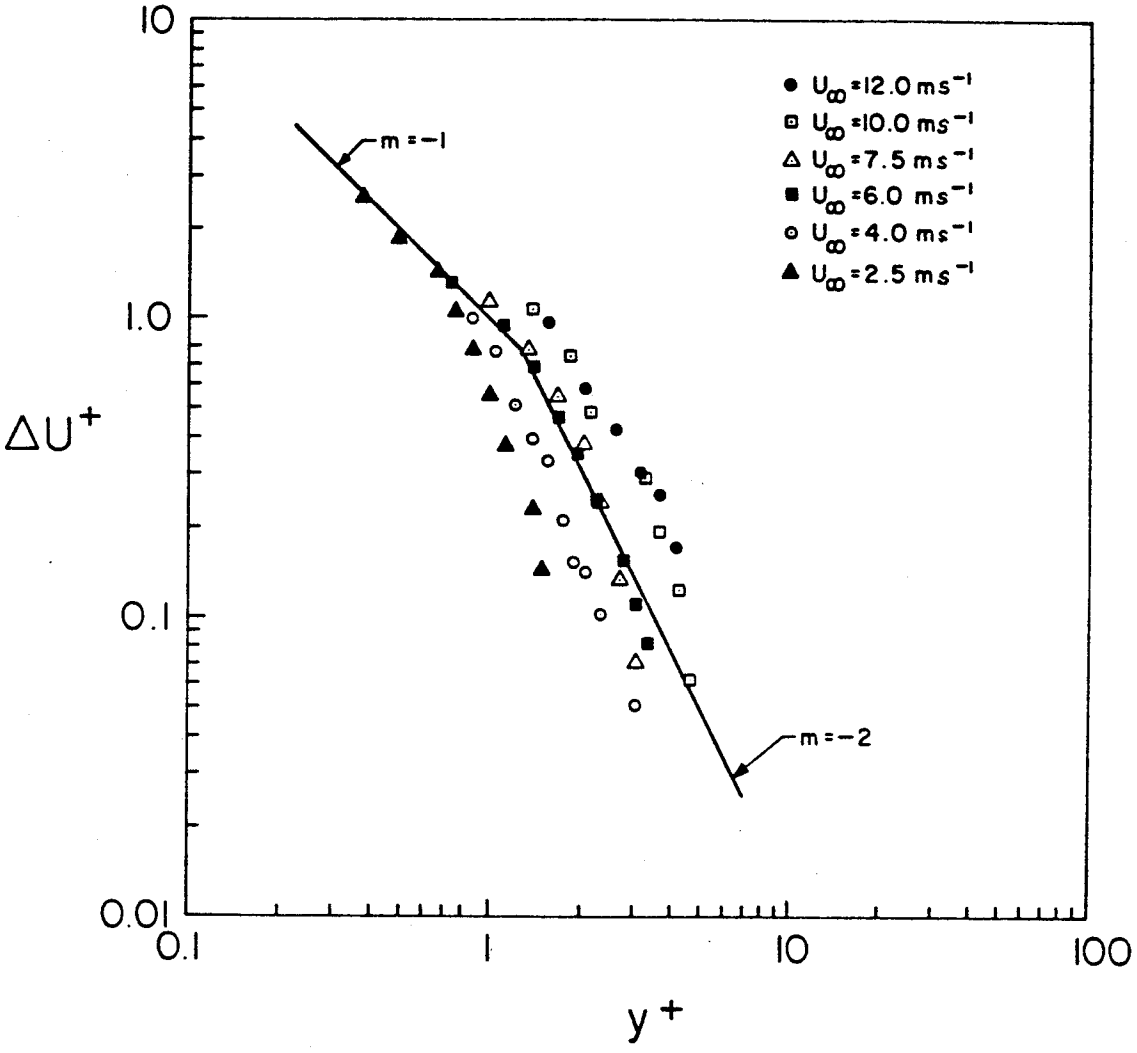

Figure 9. The deviation of the measured velocity distribution from $U^+ = Y^+$ curve in the region where the wall effect is significant.

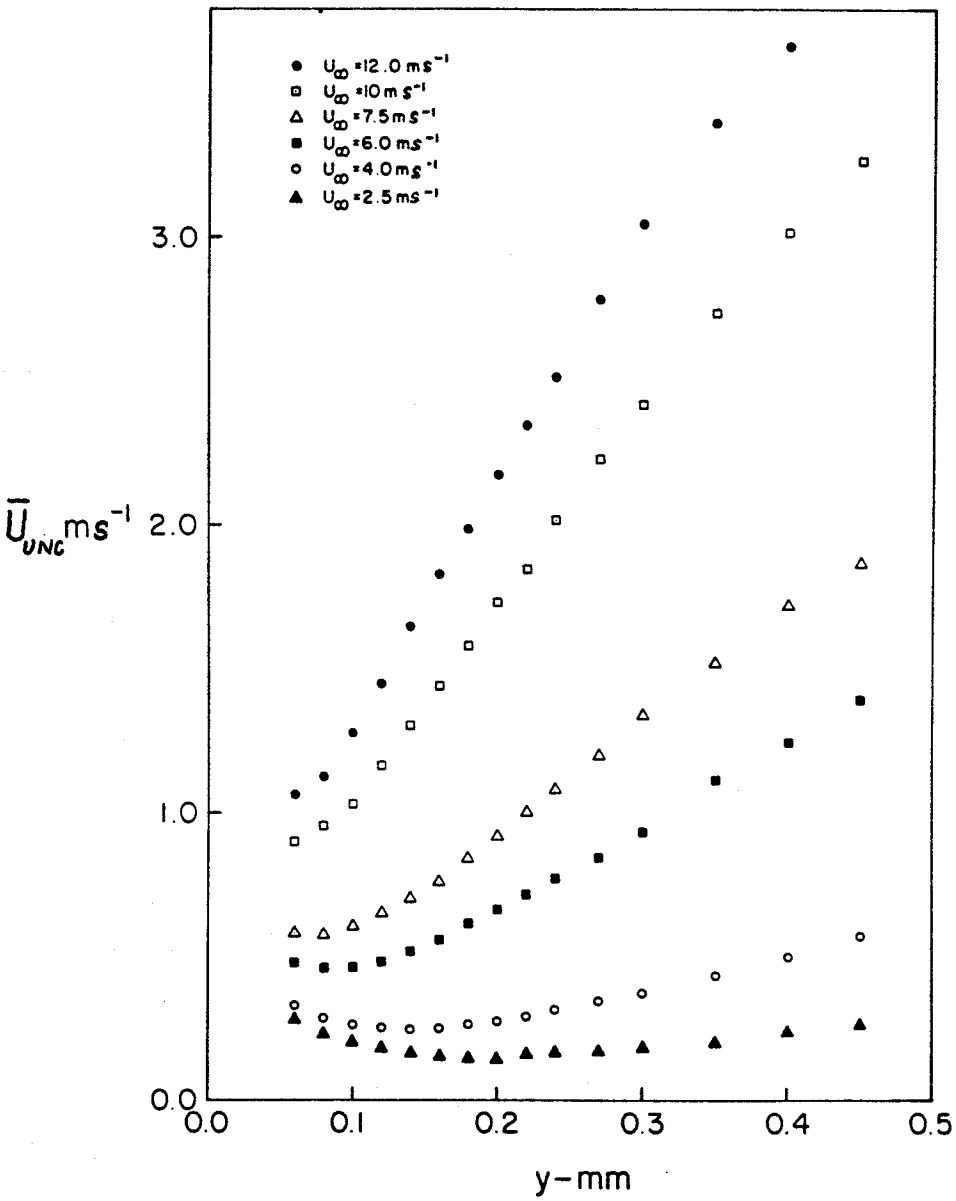

Figure 10. Uncorrected velocity distribution in sub-layer.

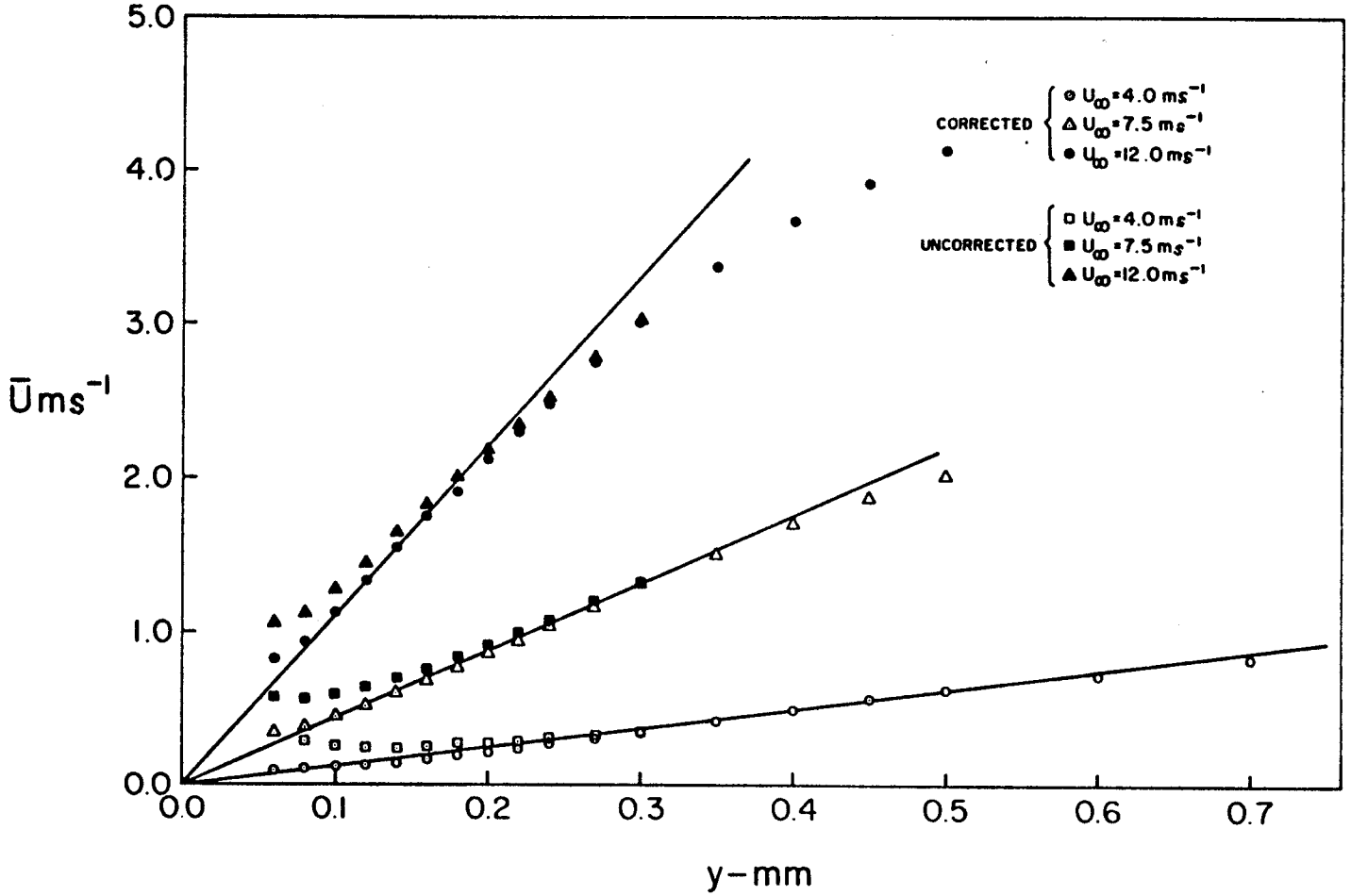

Figure 11. Corrected and uncorrected velocity profile in sub-layer.

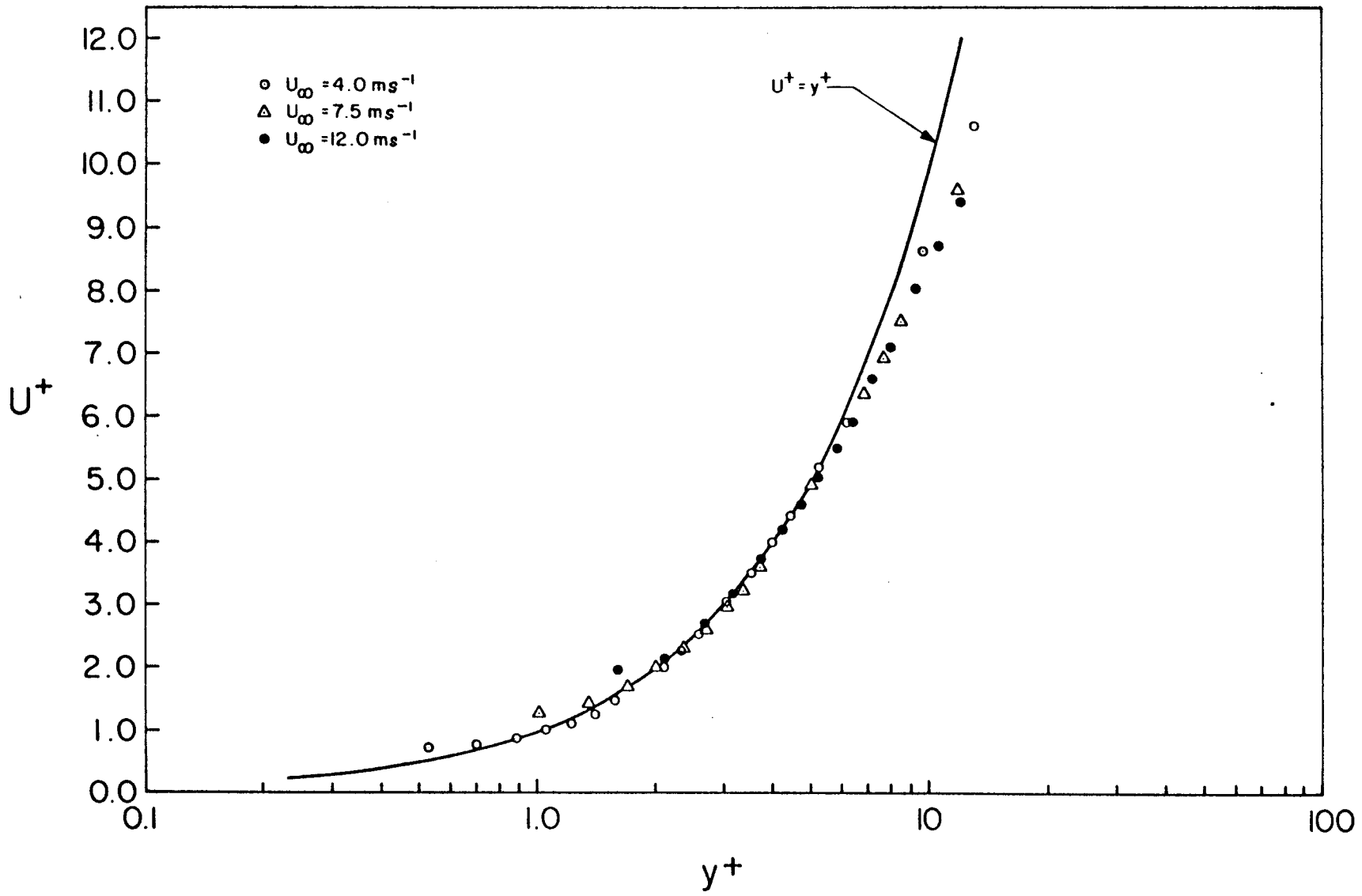

Figure 12. Corrected velocity profile in sub-layer.

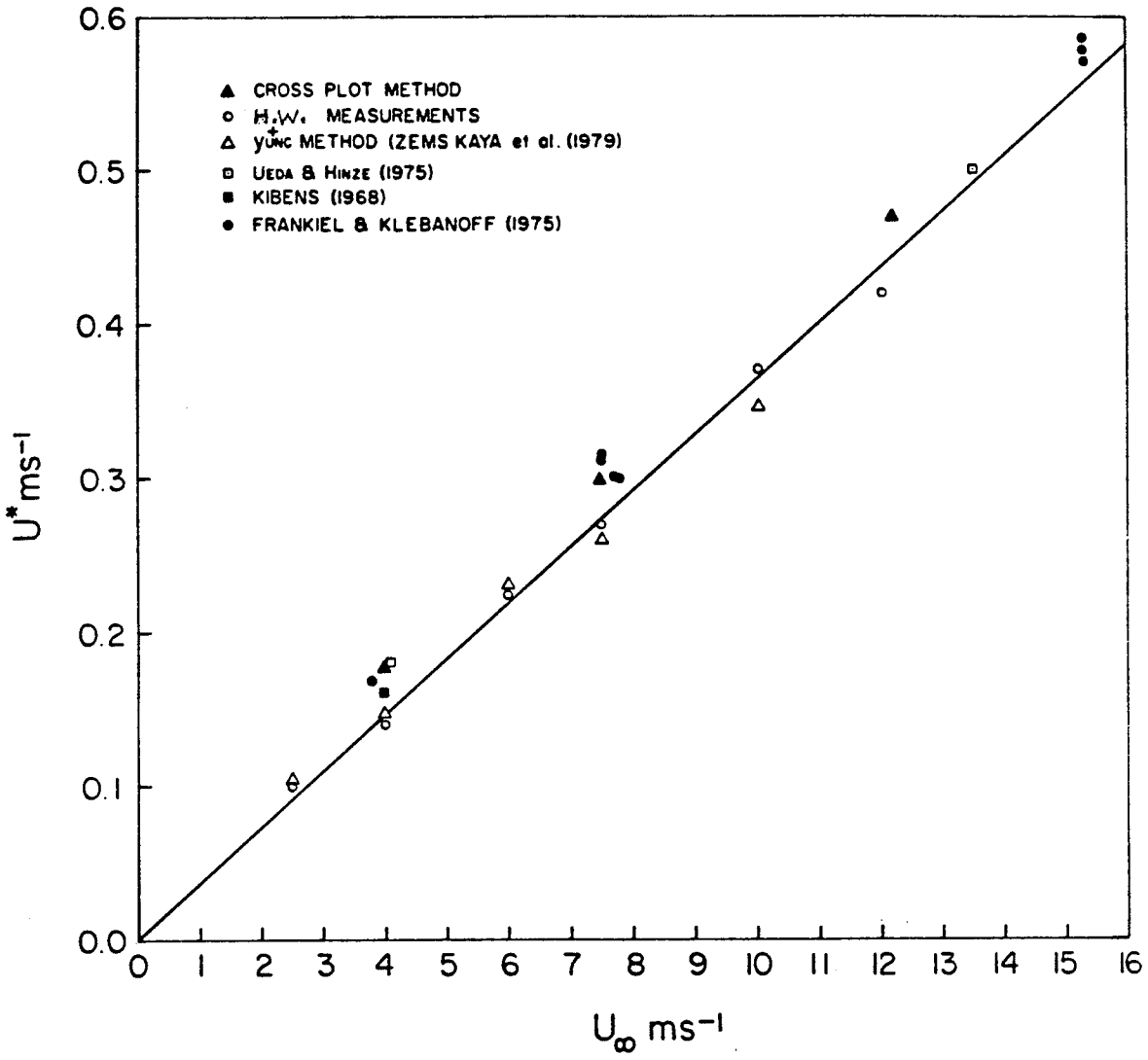

Figure 13. Comparison of friction velocity measurements.

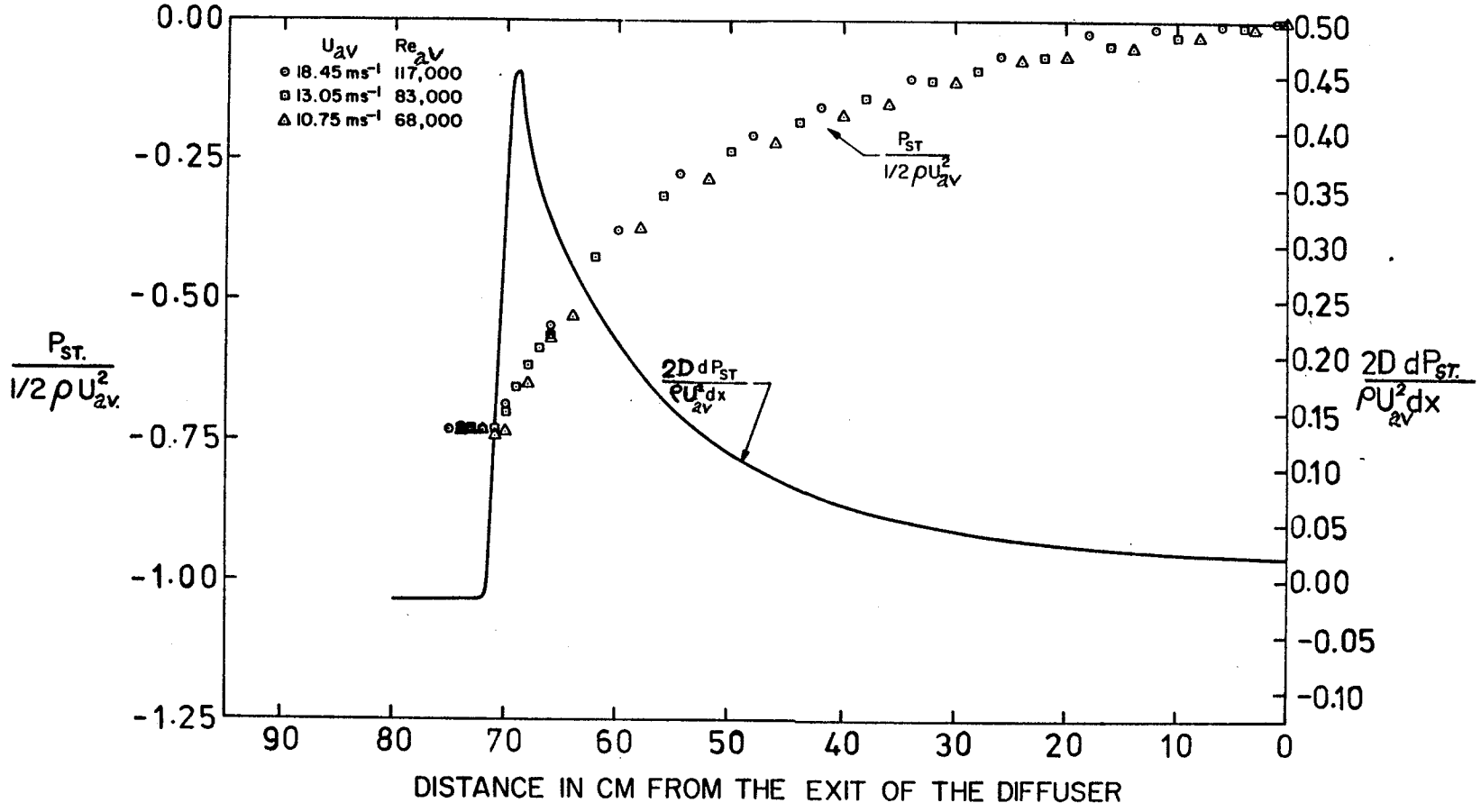

Figure 14. Static pressure distribution and static pressure derivative along the length of the diffuser.

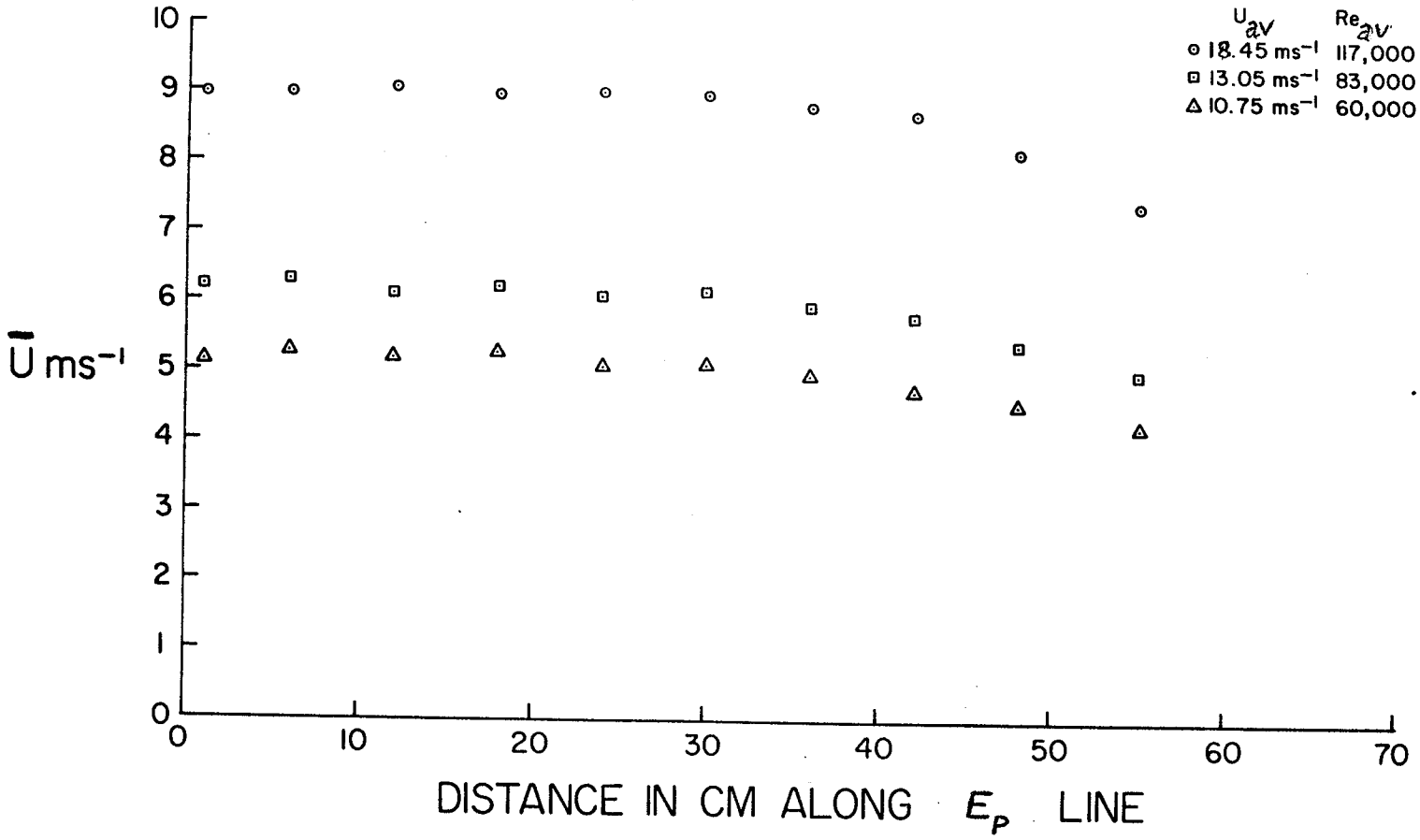

Figure 15. Mean velocity measurements along the energy peak line.

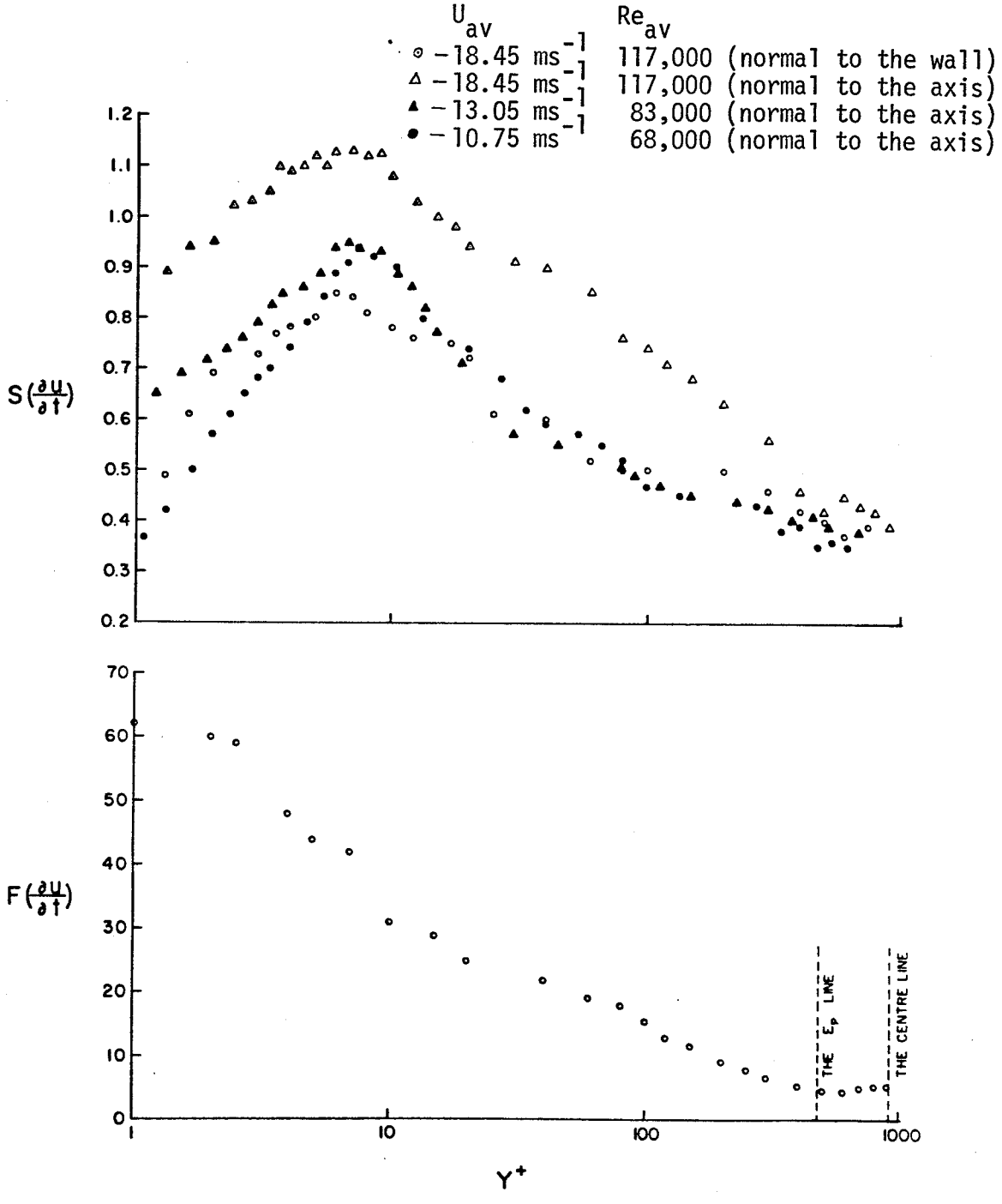

Figure 16. Skewness and flatness of ∂u/∂t in Diffuser flow.

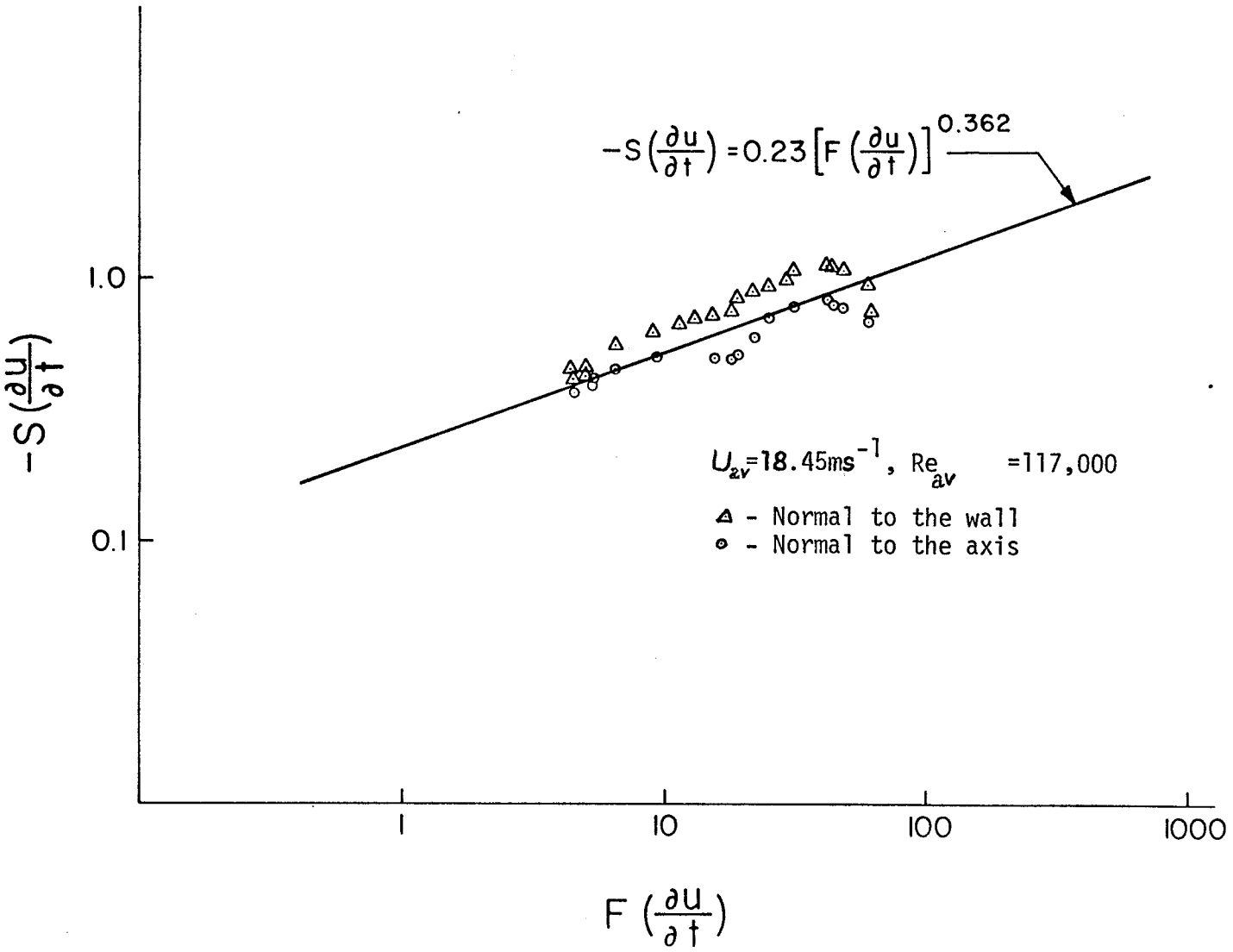

Figure 17. Variation of -S(∂u/∂t) with F(∂u/∂t) in diffuser flow.

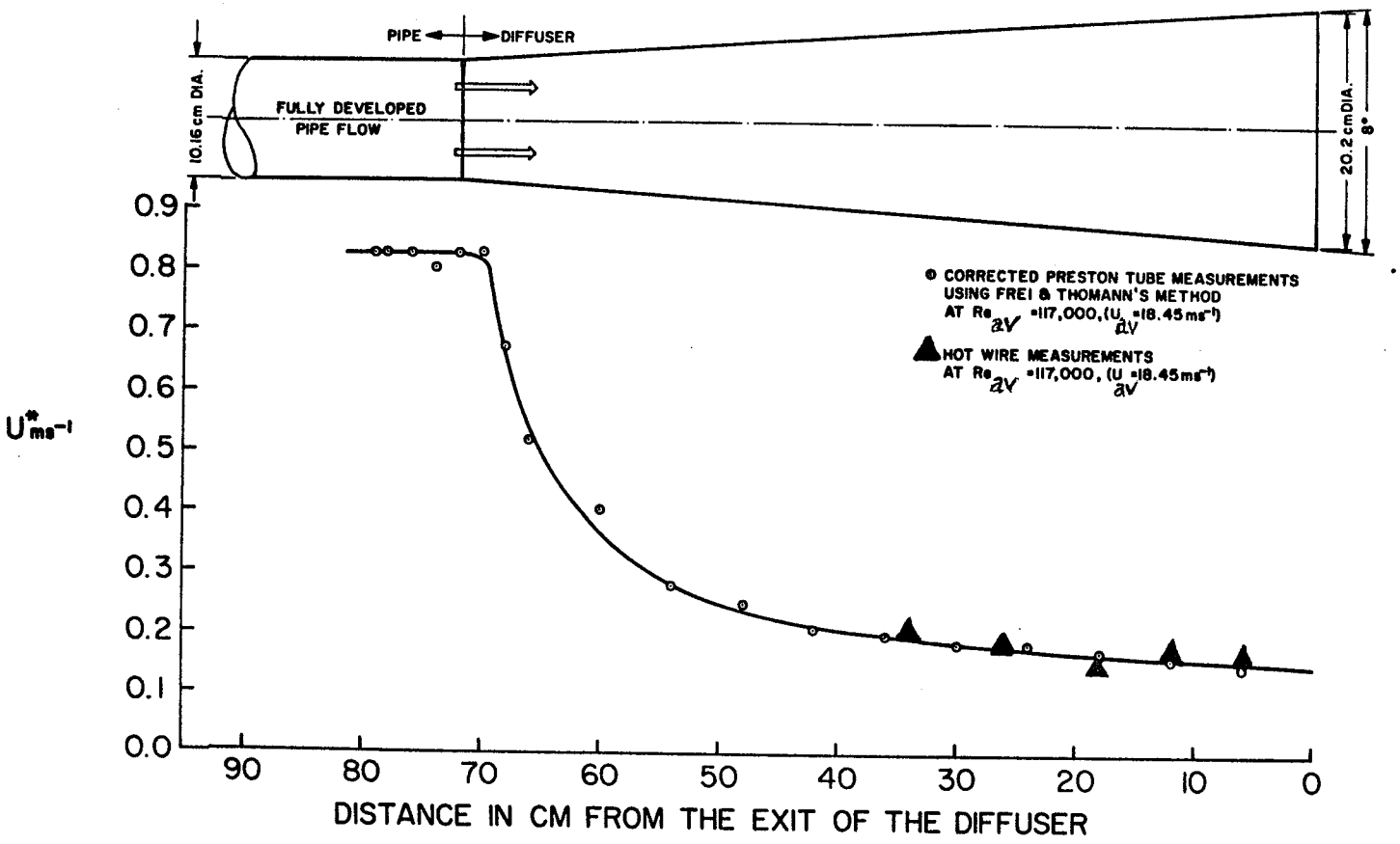

Figure 18. Corrected friction velocity measurements with hot wire and Preston tube in the diffuser.